

The British Journal of Radiology

Magnetic resonance neurography of the head and neck: state of the art, anatomy, pathology and future perspectives

--Manuscript Draft--

Manuscript Number:	BJR-D-20-00798
Full Title:	Magnetic resonance neurography of the head and neck: state of the art, anatomy, pathology and future perspectives
Article Type:	Review Article
Section/Category:	Diagnostic Radiology
Corresponding Author:	Frédéric Van der Cruyssen University Hospitals Leuven Leuven, BELGIUM
Corresponding Author Secondary Information:	
Corresponding Author's Institution:	University Hospitals Leuven
Corresponding Author's Secondary Institution:	
First Author:	Frédéric Van der Cruyssen
First Author Secondary Information:	
Order of Authors:	Frédéric Van der Cruyssen Tomas-Marijn Croonenborghs Tara Renton Robert Hermans Constantinus Politis Reinhilde Jacobs Jan Casselman
Order of Authors Secondary Information:	
Abstract:	Magnetic resonance neurography allows for the selective visualization of peripheral nerves and is increasingly being investigated. Whereas in the past the imaging of the extracranial cranial and occipital nerve branches was inadequate, more and more techniques are now available that do allow nerve imaging. This basic review provides an overview of the literature with current state of the art, anatomical landmarks and future perspectives. Furthermore, we illustrate the possibilities by means of a few case studies.
Suggested Reviewers:	Kaan Orhan call53@yahoo.com Philippe Demaerel philippe.demaerel@uzleuven.be Vincent Vandecaveye vincent.vandecaveye@uzleuven.be Egon Burian egon.burian@tum.de
Opposed Reviewers:	

Title: Magnetic resonance neurography of the head and neck: state of the art, anatomy, pathology and future perspectives

Short Title: Magnetic resonance neurography of the head and neck

Invited review

Authors

Dr. Frédéric Van der Cruyssen^{1,2}

Dr. Tomas-Marijn Croonenborghs^{1, 2}

Prof. Dr. Tara Renton³

Prof. Dr. Robert Hermans⁴

Prof. Dr. Constantinus Politis^{1,2}

Prof. Dr. Reinhilde Jacobs^{2,5,6}

Prof. Dr. Jan Casselman^{7,8,9}

Affiliations

¹Department of Oral & Maxillofacial Surgery, University Hospitals Leuven, Leuven, Belgium

²OMFS-IMPACT Research Group, Department of Imaging and Pathology, Faculty of Medicine, University Leuven, Leuven, Belgium

³Department of Oral Surgery, King's College London Dental Institute, London, United Kingdom

⁴Department of Radiology, University Hospitals Leuven, Leuven, Belgium

⁵Department of Oral Health Sciences, KU Leuven and Department of Dentistry, University Hospitals Leuven, Leuven, Belgium

⁶Department of Dental Medicine, Karolinska Institutet, Stockholm, Sweden

⁷Department of Radiology, AZ St-Jan Brugge-Oostende, Bruges, Belgium

⁸Department of Radiology, AZ St-Augustinus, Antwerp, Belgium

⁹Department of Radiology, UZ Gent, Gent, Belgium

Corresponding Authors

Frédéric Van der Cruyssen
Department of Oral & Maxillofacial Surgery
University Hospitals Leuven
Kapucijnenvoer 33,
3000 Leuven, Belgium
Email: frederic.vandercruyssen@uzleuven.be
Tel.: +32 16 33 24 62

Jan Casselman
Department of Radiology
AZ Sint-Jan
Ruddershove 10,
8000 Bruges, Belgium
Email: jan.casselmann@azsintjan.be
Tel.: +32 50 45 21 01

Abstract: 76 words

Full text: 4144 words

Figures: 12

Tables: 1

Conflicts of interest

None to declare

Funding

None to declare

Acknowledgements

We would like to thank Campbell Medical Illustration for providing the art work.

Abstract

Magnetic resonance neurography allows for the selective visualization of peripheral nerves and is increasingly being investigated. Whereas in the past the imaging of the extracranial cranial and occipital nerve branches was inadequate, more and more techniques are now available that do allow nerve imaging. This basic review provides an overview of the literature with current state of the art, anatomical landmarks and future perspectives. Furthermore, we illustrate the possibilities by means of a few case studies.

1 **Title:** Magnetic resonance neurography of the head and neck: state of the art, anatomy,
2 pathology and future perspectives

3 **Short Title:** Magnetic resonance neurography of the head and neck
4
5
6

7 Abstract

8 Magnetic resonance neurography allows for the selective visualization of peripheral nerves
9 and is increasingly being investigated. Whereas in the past the imaging of the extracranial
10 cranial and occipital nerve branches was inadequate, more and more techniques are now
11 available that do allow nerve imaging. This basic review provides an overview of the literature
12 with current state of the art, anatomical landmarks and future perspectives. Furthermore, we
13 illustrate the possibilities by means of a few case studies.
14
15
16
17
18

19 Introduction

20 Magnetic resonance neurography (MRN) refers to dedicated MRI sequences that selectively
21 enhance the visualization of peripheral nerves. Several techniques have been described in the
22 literature including 2D and 3D T2 weighted fat suppressed and diffusion weighted imaging.¹
23 The first reports on MRN date from 1992 by Howe and Filler and have much evolved since
24 then.² At present, MRN is gaining importance due to the introduction of high-field MRI devices
25 and improved imaging techniques.
26
27
28
29

30 The skull base course of cranial nerve MRI anatomy has been extensively reviewed.³⁻⁶ In this
31 article we will review the state of the art and relevant MRN anatomy of the extracranial cranial
32 and occipital nerve branches with illustrative pathologic cases. Finally, we will discuss some
33 future directions.
34
35
36

37 State of the art

38 Although there is well supported literature on MRN in musculoskeletal imaging, the original
39 research articles are rather limited for the head-neck area. There are several factors why MRN
40 is more difficult to implement in this region. First, the cranial nerves have small calibers and
41 have a complex tortuous course, passing tissues with very different physical properties. The
42 close proximity of fat pads, sinuses and vessels with slow and fast flows require more
43 performant sequences. Ideally a cranial nerve MRN sequence has a large FOV with three-
44 dimensional thin slice thickness, high signal- (SNR) and contrast-to-noise ratios (CNR), with
45 uniform fat, venous and arterial suppression and minimal magic angle artefacts. All these
46 requirements should be met within reasonable acquisition times and minimum chance for
47 motion artefacts. Also, when considering nerve-related pathology we can expect surgical and
48 pathology induced susceptibility artefacts such as edema, increased vascularity and metal
49 particles, which should be accounted for when possible. Previous reports described cranial
50 nerve anatomy using various MRI sequences such as 3D bFFE (3D balanced fast-field echo
51 sequences), T2w TSE (turbo spin echo), STIR (short tau inversion recovery) and CISS
52 (constructive interference in steady state).^{3-5,7} Although these sequences nicely demonstrate
53
54
55
56
57
58
59
60
61
62
63
64
65

1 the anatomy, they are not nerve-specific as surrounding structures are not suppressed. In true
2 MRN sequences we try to obtain a heavily T2 weighted image to achieve high soft tissue
3 contrast with homogenous fat, arterial and venous suppression. Several authors published on
4 available techniques for inferior alveolar, lingual, as well as occipital nerve imaging mainly
5 based on 3D PSIF (reversed fast imaging in steady-state free precession).^{8,9} PSIF combines a
6 steady state with a water excitation pulse and fat suppression, selectively enhancing neural
7 anatomy with excellent vascular suppression. A disadvantage of PSIF is the lower SNR and risk
8 for susceptibility artefacts compared to STIR sequences (**Figure 1**). A protocol suggested by
9 Chhabra et al. is further complemented by STIR, CISS, bFFE and DTI (diffusion tensor imaging).⁹
10 By adding multiple sequences, one reduces the risk of non-diagnostic images but loses time
11 and cost efficiency, which are becoming increasingly important in a healthcare environment
12 under financial pressure and with increasing demand for MRI. The authors apply the 3D CRANI
13 (CRANial Nerve Imaging) sequence which is based on contrast enhanced black blood 3D STIR
14 TSE preceded by an MSDE (motion-sensitized driven equilibrium) pulse in combination with a
15 pseudo steady state sweep and compressed sensing.^{10,11} Advantages of 3D CRANI are high
16 SNR and CNR and less susceptibility artefacts. By combining 3D PSIF and 3D CRANI, a cranial
17 MRN examination can be performed in a total acquisition time of 12 minutes. **Table 1**
18 describes in detail the author's MRN protocol including 3D PSIF and 3D CRANI sequences.
19 Routine T1, T2w and 3D FLAIR (fluid attenuated inversion recovery) brain sequences could be
20 added as well to exclude intracranial pathology. DTI is increasingly being used but, for the time
21 being, mostly remains of scientific value.^{10,12,13} In order to obtain a diagnostic MRN acquisition,
22 adequate patient positioning and coil selection is necessary.⁶ Thorough patient fixation in mild
23 hyperextension using a 32 channel head coil plays an important role in optimization of the
24 SNR (**Figure 2**). Others have advocated the use of a 16 channel head neck spine coil.¹⁴ Finally,
25 post-processing using maximum intensity projection (MIP) and multiplanar reformatting
26 (MPR) renders the necessary viewing windows to evaluate the attenuation-enhanced cranial
27 nerves along their trajectory or in non-axial planes according to the radiologist's discretion
28 (**Figure 3**).^{15,16}

29 In the next paragraphs the cranial and occipital nerve imaging anatomy is described and
30 further illustrated by a supplementary **video**.

46 Trigeminal Nerve

47 Anatomy

48 The trigeminal nerve splits into three main divisions before it leaves the skull: ophthalmic
49 nerve (V₁), maxillary nerve (V₂) and mandibular nerve (V₃). The ophthalmic division (V₁) splits
50 into three branches (lacrimal, frontal and nasociliary nerve) which enter the orbit via the
51 superior orbital fissure. The maxillary division (V₂) leaves the cranial cavity via the foramen
52 rotundum and reaches the pterygopalatine fossa. It innervates the teeth of the upper jaw and
53 part of the nasal mucosa. Its dermal branches, the zygomatic nerves and infraorbital nerve,
54 enter via the inferior orbital fissure. The infraorbital nerve runs over the floor of the orbit, it
55 passes through the infraorbital foramen to the skin of the lower eyelid, the side of the nose
56
57
58
59
60
61
62
63
64
65

1 and part of the upper lip. Preganglionic parasympathetic fibers originate from the facial
2 nerve. They are conveyed via the greater petrosal nerve. The latter branches off at the knee
3 level of the facial nerve (geniculum), located in the petrosal bone and runs over an intracranial
4 sulcus of the same name on the top of the petrosal bone to the foramen lacerum. The
5 postganglionic (ortho)sympathetic fibers originate from the superior cervical ganglion. They
6 leave the internal carotid plexus as the deep petrosal nerve. In the cartilage of the foramen
7 lacerum they join to form the Vidian nerve in the Vidian canal. Via this canal it reaches the
8 pterygopalatine fossa and its ganglion. Postganglionic nerves leave for the nasal cavity (via the
9 foramen sphenopalatinum), to the palate (via nervus palatinus major and nervus palatini
10 minores through channels of the same name) to the pharynx and also to the orbit. They supply
11 the mucosa and glands of the nose, palate and part of the pharynx (**Figure 4**).
12
13
14
15
16

17 The mandibular nerve (V_3) runs through the foramen ovale from the middle cranial fossa to
18 the infratemporal fossa. Three of its four large branches (buccal nerve, inferior alveolar nerve
19 and auriculotemporal nerve) reach the lower skin of the face and are responsible for the
20 cutaneous innervation of the face but it also carries the smaller motor part (radix motoria)
21 which supplies the muscles of mastication. Approximately one centimeter below the foramen
22 ovale, the trunk of the mandibular nerve splits into an anterior and a posterior division. Its
23 branches are described in three groups (trunk, anterior and posterior division). Branches of
24 the trunk of the mandibular nerve include: the medial pterygoid nerve for the chewing muscle
25 of the same name, meningeal rami which innervate the meninges that runs through the
26 foramen spinosum together with middle meningeal artery.
27
28
29
30
31

32 Branches of the anterior division are all motoric except the buccal nerve which appears
33 between the two heads of lateral pterygoid muscle (**Figure 5**). It innervates a postage stamp
34 large area on the inside and outside of the cheek. The masseteric nerve runs superior from
35 the lateral pterygoid muscle. It passes between the tendon of temporal muscle and the
36 temporomandibular joint (TMJ) and reaches the masseter muscle via the mandibular incisura.
37 On the way, it supplies small branches towards the TMJ. The deep temporal branches, two or
38 three in number, run over the lateral pterygoid muscle to innervate the temporal muscle. The
39 lateral pterygoid nerve innervates the muscle of the same name.
40
41
42
43
44

45 The posterior division of the mandibular nerve constitutes the auriculotemporal, lingual,
46 inferior alveolar and mylohyoid nerve (**Figure 5, 6**). The auriculotemporal nerve innervates
47 most of the temporal region and a small part of the auricle (leading edge) and the outer ear
48 canal. In the classical case it "embraces" the middle meningeal artery. Then, together with the
49 maxillary artery, it runs backwards between the sphenomandibular ligament and the
50 mandibular collum, turns around the condyle of the mandible and ends up in the
51 subcutaneous membrane of the temporal region. Secretomotor fibers originating from the
52 otic ganglion are transported to the parotid gland via this nerve. The lingual nerve appears in
53 the infratemporal fossa between both pterygoid muscles and runs antero-inferiorly over the
54 lateral side of medial pterygoid muscle. It innervates the mucosa of the anterior two thirds of
55 the tongue, the mucosa of the oral floor and of the lingual side of the gums. It also carries the
56
57
58
59
60
61
62
63
64
65

1 taste fibers from the anterior tongue and parasympathetic preganglionic fibers for the
2 submandibular ganglion (intended for the submandibular and sublingual glands). The
3 preganglionic parasympathetic fibers originate from the facial nerve and reach the lingual
4 nerve via the chorda tympani, which joins high up in the infratemporal fossa. The inferior
5 alveolar nerve also ends up between the two pterygoid muscles in the infratemporal fossa.
6 There, it lies behind the lingual nerve. Together with the artery of the same name it runs
7 between the sphenomandibular ligament towards the inferior alveolar canal or mandibular
8 canal. Just before it enters the mandibular foramen, it releases the mylohyoid nerve that
9 innervates the mylohyoid muscle and anterior belly of the digastric muscle. The inferior
10 alveolar nerve innervates all the teeth of the lower jaw (inferior dental rami, dental plexus),
11 the adjacent gums (inferior gingival rami) and, via its end branch (mental nerve), the skin of
12 the chin (mental rami) and the skin and mucosa of the lower lip (inferior labial rami).¹⁷⁻¹⁹

19 *Imaging*

20 The brainstem, cisternal and cavernous trigeminal segments can be imaged using
21 conventional brain sequences including CISS and balanced FFE sequences and have been
22 extensively reviewed in the past.^{6,20} The peripheral trigeminal nerve branches are best viewed
23 in multiple planes after thick-slab MIP. The first (V_1), second (V_2) and anterior division of the
24 third division (V_3) can be well depicted on axial views whereas the lingual and inferior alveolar
25 nerve are best seen in a coronal oblique direction (**Figure 4, 5, 6**).

26 In addition to the neurovascular conflict seen in trigeminal neuralgia cases, more and more
27 neurological abnormalities are becoming detectable. The branches that are mostly involved
28 in pathological conditions are the lingual and inferior alveolar nerve. Their course makes these
29 nerves vulnerable to numerous dental and oro-maxillofacial procedures. MRN techniques can
30 aid in grading and clinical decision making if trauma has occurred.²¹ Interested readers are
31 referred to a recent systematic review summarizing the available knowledge base on MRN in
32 post-traumatic trigeminal neuropathies.²² There is also increasing interest for the use of MRN
33 in orofacial pain patients and more specifically in migraine and trigeminal autonomic
34 cephalalgia (**Figure 4**).²³

44 *Facial Nerve*

45 The facial nerve consists out of motor, sensory and parasympathetic fibers. The sensory fibers
46 innervate a part of the inner ear and the special sensory fibers transport the taste stimuli from
47 the anterior two thirds of the tongue via the chorda tympani. The parasympathetic fibers
48 innervate the submandibular, sublingual and minor salivary glands, as well as the lacrimal
49 glands. The motor fibers innervate the muscles responsible for the facial expression.

50 The primary or cisternal segment of the facial nerve leaves the brainstem close to the dorsal
51 pons, transverses the cerebellopontine angle and enters the temporal bone by the porus
52 acousticus in proximity to the vestibulocochlear nerve branches: superior to the cochlear
53 nerve and anterior to the superior and inferior vestibular nerves. The trajectory through the

1 temporal bone is subdivided in a meatal, labyrinthine, tympanic and mastoid segment. The
2 sensory fibers, coming from the intermediate nerve, give on the one hand sensibility to the
3 posterior concha and external auditory canal, on the other hand the special sensory fibers will
4 form the chorda tympani.
5
6

7 The main trunk of the facial nerve leaves skull base via the stylomastoid foramen, it
8 immediately releases the smaller posterior auricular r. auricularis. Subsequently, the nerve
9 enters the craniomedial part of the parotid gland. Over the intraglandular course the nerve
10 subdivides into five branches, which appear separately at the upper, front and lower edges of
11 this gland. These end branches spread from here to the facial mimic muscles like the spread
12 fingers of a hand resting on the parotid area (temporal, zygomatic, buccal, marginal
13 mandibular and cervical, **Figure 6**).^{24,25}
14
15
16
17
18

19 *Imaging*

20 When considering MRI-imaging of the facial nerve, two segments need to be distinguished
21 from each other: the skull base and the extracranial nerve segments. The intracranial and the
22 temporal facial nerve segment is best visualized using 3D CISS, axial T1-weighted and fat-
23 suppressed T2-weighted images.²⁶ Visualization of the facial nerve within the stylomastoid
24 canal, the extracranial and intraparotid part of the VII cranial nerve can be made using thick-
25 slab MIP/MPR reconstructions of 3D PSIF, and in case of extensive artefacts a black blood 3D-
26 STIR such as 3D CRANI.⁹ In case of nerve pathology, an increase of signal intensity and nerve
27 caliber changes can be identified (**Figure 7**). The use of a 3D PSIF sequence in combination
28 with microsurface coils resulted in superior visualization of the peripheral facial nerve
29 branches, in comparison to a standard head and neck coil, as was reported by Chu et al.²⁷ The
30 3D-DESS-WE (double-echo steady state with water excitation) sequence is another
31 established option to be considered for peripheral facial nerve neurography.²⁸⁻³⁰
32
33
34
35
36
37
38
39

40 *Cranial nerves IX to XII*

41 The trajectory of the IX, X and XII cranial nerves is anatomically closely intercalated, moreover
42 a lot of imaging characteristics are similar and therefore they are discussed together (**Figure**
43 **8**).
44
45
46

47 *Glossopharyngeal nerve anatomy*

48 The glossopharyngeal nerve or IX cranial nerve is composed of a combination of motor,
49 sensory and parasympathetic fibers. Firstly, the sensory, gustatory and visceral stimuli are
50 transported via afferent fibers from the retroauricular region, the posterior third of the
51 tongue, the pharynx wall and the tonsils, the soft palate and the eardrum. Secondly, the motor
52 efferents innervate the stylopharyngeus muscle. Thirdly, the parasympathetic fibers stimulate
53 the production of saliva within the parotid gland.³¹
54
55
56
57
58
59
60
61
62
63
64
65

1 The origin of the IX cranial nerve is strongly associated with the vagus nerve, sharing three
2 functional nuclei in the upper medulla oblongata. The nerve branches from the medulla
3 oblongata within the cerebellomedullary cistern, slightly superior to the vagus nerve. The 9th,
4 10th and 11th cranial nerves course in an anterolateral direction through the cistern to the
5 jugular foramen, exiting the foramen anteriorly from the internal jugular vein. Within the
6 foramen the glossopharyngeal nerve is known for two focal expansions: a superior node
7 handling general sensible information and a lower node handling visceral sensory, taste and
8 carotid innervations. The extratemporal course of the IX cranial nerve continues in a caudal
9 direction within the carotid space and disperses in 5 major branches. Firstly, the tympanic
10 nerve branches from the inferior node, carrying sensory information from the external and
11 middle ear and parasympathetic stimuli to the parotid gland via the lesser petrosal nerve.
12 Secondly, the stylopharyngeus branch gives motor input to the stylopharyngeus muscle.
13 Thirdly, the pharyngeal branches associate with branches from the vagus nerve, forming the
14 pharyngeal plexus. Fourthly, the carotid sinus branch mediates parasympathetic information
15 to the carotid body. Finally, the lingual branch conveys general and gustatory sensory input
16 from the posterior third of the tongue.^{31,32}

25 *Vagus nerve Anatomy*

26 The n. X forms the pharyngeal plexus and mediates the motor function of the soft palate. The
27 parasympathetic fibers of the dorsal motor core of the n. X innervate pharynx, esophagus,
28 trachea, bronchi, lungs, heart, intestines, liver and pancreas.

31 Multiple rootlets exiting the ventrolateral sulcus, formed by the olive and interior cerebellar
32 peduncle, fuse together in the vagus nerve. The vagus and glossopharyngeal nerve progress
33 closely intercalated through the cerebellopontine angle. Noteworthy, is the small meningeal
34 branch coming from the vagus nerve, innervating the dura within the posterior cranial fossa.
35 Subsequently, the vagus nerve travels through the center of the jugular foramen: superficial
36 to the internal jugular vein and caudal to the glossopharyngeal nerve. Caudally progressing
37 within the carotid space between, however slightly posterior to the internal carotid artery and
38 internal jugular vein. The internal jugular vein remains lateral and superficial to the vagus
39 nerve; the common carotid artery travels medial and slightly anterior to the nerve.

42 There are four major extracranial branches leaving the vagus nerve in the head and neck area.
43 Firstly, the auricular branch or Arnold nerve, exiting from the main nerve when passing
44 through the jugular foramen, this nerve receives sensory input coming from the external
45 auditory canal and tympanic membrane. Secondly, the pharyngeal branches leave the vagus
46 nerve below the skull base and form, together with the IX cranial nerve, the pharyngeal plexus
47 innervating the muscles of the soft palate and pharynx. Besides the motor function, the plexus
48 conveys sensory stimuli coming from the epiglottis, trachea and esophagus. Thirdly, the
49 superior laryngeal nerve has a sensory, as well as a motor component. The internal sensory
50 branch conducts sensory input from the hypopharynx, larynx and vocal cords, the external
51

1 motor branch innervates the cricothyroid and inferior pharyngeal constrictor muscles. And
2 finally, the recurrent laryngeal nerve (RLN) is identified with its renowned asymmetrical
3 anatomical morphology. Bilaterally the RLN branches from the vagus nerve, it loops around
4 the subclavian artery on the right side and on the left side around the aortic arch. The RLN
5 mediates somatic and visceral sensory input coming from below the vocal cords, moreover,
6 conveying motor output to all laryngeal musculature with exception of the cricothyroid
7 muscle. Hereafter, the vagus nerve continues the trajectory into the thorax.^{6,33,34}
8
9

10 11 *Accessory nerve Anatomy*

12 The accessory nerve solely contains motor fibers, innervating the sternocleidomastoid as well
13 as the trapezius muscle. The accessory nerve is composed from of both cranial and spinal (C1-
14 5) rootlets. The main trunk of the accessory nerve subsequently travels in a lateral direction,
15 before the nerve leaves the skull via the jugular foramen wherein connections with the vagus
16 nerve can be found. The extracranial accessory nerve runs through the center of the carotid
17 space between the medial internal carotid artery and laterally positioned internal jugular vein
18 (IJV). Subsequently, the nerve divides again in the cranial and spinal roots. The cranial rootlets
19 or internal branches fuse together with the vagus nerve and the spinal rootlets or external
20 branches laterally cross the IJV, passing the transverse process of atlas mostly anteriorly and
21 advancing medially from the styloid process and digastric and stylohyoid muscles. Further
22 progression of the nerve follows an anterolateral direction before reaching the
23 sternocleidomastoid muscle and subsequent formation of a nerve plexus with the ventral rami
24 of C2 to C4, mediating the innervation of the trapezius muscle.³⁵⁻³⁷
25
26
27
28
29
30
31
32
33

34 *Hypoglossal nerve anatomy*

35 The hypoglossal nerve is a purely motor nerve, innervating the extrinsic and intrinsic
36 musculature of the tongue, with exception of the palatoglossus muscle. The XII cranial nerve
37 is formed by two bundles of 10-15 rootlets coming from the ventrolateral sulcus at the
38 medulla oblongata. The bundles pierce through the dura mater separately and fuse together
39 after passing through the hypoglossal canal. The extracranial hypoglossal nerve is joined by
40 efferent C1 motor fibers and progresses laterally and inferiorly to the vagus nerve and internal
41 carotid artery, initially closely associated with the carotid space. Subsequently, after passing
42 the occipital artery the hypoglossal nerve will turn and mostly pass through the space between
43 carotid arteries and internal jugular vein. After progressing medially to the hyoid tendon of
44 the digastric muscle, the nerve will enter the submandibular space medial to the
45 submandibular gland and hyoglossus muscle (**Figure 9**). Some of the C1-fibers branch off more
46 cranially and innervate the superior root of the ansa cervicalis, however other C1 nerve fibers
47 conveying motor input for the geniohyoid and thyrohyoid muscles will remain associated with
48 the XII cranial nerve.^{32,38,39}
49
50
51
52
53
54
55
56
57

58 *Glossopharyngeal, vagus, accessory and hypoglossal nerve imaging*

59
60
61
62
63
64
65

1 Evaluation of the cisternal IX, X and XI cranial nerve segments is preferably performed using
2 heavily T2-weighted steady-state free precession imaging sequences.²⁶ However, these 2-D
3 sequences have mainly been replaced by 3D CISS and 3D FIESTA.³ The distinct foramina nerve
4 segments are identified using conventional 3D FIESTA, or CE-MRA (contrast-enhanced
5 magnetic resonance angiograph) as described by Linn et al.^{5,40} The below-skull-base related
6 nerve segments can be nicely differentiated on the MIP/MPR-reformatted 3D CRANI images
7 (**Figure 8,9**). They are conveniently identified on coronal and axial planes. As discussed by
8 Chhabra and colleagues, 3D PSIF is also a valuable technique for neurography of these closely
9 intercalated cranial nerves.²¹ The typical nerve trajectories can be distinguished as follows,
10 the extracranial vagus nerve is positioned between the medial IX and lateral XII nerve and has
11 the largest diameter.
12
13
14
15
16
17
18
19
20
21
22
23
24
25
26
27
28
29
30
31
32
33
34
35
36
37
38
39
40
41
42
43
44
45
46
47
48
49
50
51
52
53
54
55
56
57
58
59
60
61
62
63
64
65

Occipital Nerves (C2)

Anatomy

The greater occipital nerve (GON) ensues from the fusion of nerve fibers coming from the medial branch of the dorsal ramus of the second and, to a lesser degree, the third spinal nerve. At the level of the C1-C2 vertebrae the nerve travels in the occipital direction between the medial inferior capitis oblique and lateral semispinal muscles. Important anatomical variation is described concerning the penetration of the trapezius, semispinalis capitis and inferior capitis oblique muscles which are pierced by GON in respectively, 45%, 7,5% and 90% of cases.⁴¹ Next, the nerve loops upwards, joins the occipital artery and subdivides in a medial and lateral branch before terminal branches ensue.⁴¹⁻⁴⁴

The lesser occipital nerve (LON) typically originates from the ventral rami of spinal nerves C2 and C3. The nerve loops around the sternocleidomastoid muscle (SCM). Its trajectory is parallel to the posterior border of the SCM, piercing the superficial lamina of the cervical fascia, in direction of the occipital area. Finally, the LON divides into medial and lateral branches in the middle between the intermastoid line and inion. Interconnections or overlap of GON and LON twigs are frequently present.⁴³⁻⁴⁵

The third occipital nerve (TON) derives from the superficial medial branch of the dorsal ramus of the third spinal nerve. The nerve courses on top of the dorsolateral surface of the C2-C3 facet joint. The TON travels deeply to the semispinalis capitis muscle in a posterior direction when a communicating branch to GON exits. The overlying musculature will be pierced by TON before progressing subcutaneously.^{34,41,43,44}

Functionally, GON, LON and TON receive somatic sensory input from the occipital region. The semispinalis muscle will receive motor output via GON, and to a lesser degree from TON (**Figure 10**).^{34,43,44}

Imaging

The occipital nerves are easily visualized on a slightly oblique axial plane using 3D PSIF or 3D CRANI sequences and are of increasing interest to neurologists and pain specialists. Pathological thickening and signal alterations can be noted in cases of occipital neuralgia also referred to as occipital migraine.²³ Occasionally one can also detect pathological changes after trauma or surgery in this region (**Figure 10**).

Future perspectives

MRN performance and applications are evolving rapidly. Where 0.5T systems were available 20 years ago, we are now seeing the arrival of clinical 7T and higher. The introduction of these high-field MRI devices can further improve spatial resolution and soft tissue contrast. However, there is also a risk of increasing susceptibility artefacts as they increase with increasing field strength and thus, they should not be considered the holy grail in MRN imaging. Rather a combination of high-field systems, specialized coils, improved post-processing and contrast agents will likely evolve this field in the next phase.^{27,46,47} First, there is a need to further define anatomical benchmarks for the cranial nerves. Several authors have

1 described reference values for the trigeminal nerve or provided classifications to define
2 degree of nerve injury.^{14,48} Next, there is a whole field of research left to obtain functional
3 information by means of DTI and diffusion tensor tractography (DTT). These techniques are
4 based on differences in diffusion of protons along nerve tracts and allow quantification of
5 diffusion restriction by means of the apparent diffusion coefficient (ADC) and fractional
6 anisotropy (FA) values. In combination with morphological changes a more detailed
7 description of neural dysfunction and neuroregeneration becomes reality.⁴⁹ Additionally, they
8 allow for a multiparametric and standardized approach towards nerve injuries and pathology,
9 which is currently lacking. Several studies described the successful application of DTI and DTT
10 in extraforaminal cranial nerve imaging.^{12,50-53} But, most reports only describe DTT of the
11 proximal nerve branches with varying reference values.^{51,54} DTT of the small distal cranial
12 nerve branches remains challenging and, for the time being, is mostly of scientific value.^{13,55}
13 In addition to strong diagnostic value, MRN also offers applications for planning of surgical
14 procedures. The surgeon could check in advance where the nerve is located in relation to the
15 neoplasia or when the anatomy deviates from the normal.⁵¹ Panoramic reconstructions can
16 aid in dental surgery planning (**Figure 11**).⁵⁶ Fusion with computed tomography images could
17 help with the placement of a temporomandibular joint prosthesis near these peripheral nerve
18 branches (**Figure 12**) and it is only a matter of time before artificial intelligence aids find their
19 way to the clinic.^{57,58}

20 In conclusion, the field of MRN is still in its infancy but a wide range of applications are already
21 under development. It is therefore important that radiologists and anyone involved in cranial
22 nerve pathology become familiar with these techniques and their possibilities.
23
24
25
26
27
28
29
30
31
32
33
34
35
36
37
38
39
40
41
42
43
44
45
46
47
48
49
50
51
52
53
54
55
56
57
58
59
60
61
62
63
64
65

References

1. Chhabra A, Andreisek G, Soldatos T, Wang KC, Flammang AJ, Belzberg AJ, et al. MR Neurography: Past, Present, and Future. *Am J Roentgenol*. 2011;197(3):583–91.
2. Howe FA, Filler AG, Bell BA, Griffiths JR. Magnetic Resonance Neurography. *Magn Reson Med*. 1992;28(2):328–38.
3. Blitz AM, Macedo LL, Chonka ZD, Ilica AT, Choudhri AF, Gallia GL, et al. High-resolution ciss mr imaging with and without contrast for evaluation of the upper cranial nerves. segmental anatomy and selected pathologic conditions of the cisternal through extraforaminal segments. *Neuroimaging Clin N Am [Internet]*. 2014;24(1):17–34. Available from: <http://dx.doi.org/10.1016/j.nic.2013.03.021>
4. Hiwatashi A, Yoshiura T, Yamashita K, Kamano H, Honda H. High-resolution STIR for 3-T MRI of the posterior fossa: Visualization of the lower cranial nerves and arteriovenous structures related to neurovascular compression. *Am J Roentgenol*. 2012;199(3):644–8.
5. Blitz AM, Choudhri AF, Chonka ZD, Ilica AT, Macedo LL, Chhabra A, et al. Anatomic considerations, nomenclature, and advanced cross-sectional imaging techniques for visualization of the cranial nerve segments by MR imaging. *Neuroimaging Clin N Am*. 2014;24(1):1–15.
6. Casselman J, Mermuys K, Delanote J, Ghekiere J, Coenegrachts K. MRI of the Cranial Nerves-More than Meets the Eye: Technical Considerations and Advanced Anatomy. *Neuroimaging Clin N Am*. 2008;18(2):197–231.
7. Lee JH, Cheng K, Choi YJ, Baek JH. High-resolution Imaging of Neural Anatomy and Pathology of the Neck. *Korean J Radiol [Internet]*. 2017;18(1):180. Available from: <https://synapse.koreamed.org/DOIx.php?id=10.3348/kjr.2017.18.1.180>
8. Zhang Z, Meng Q, Chen Y, Li Z, Luo B, Yang Z, et al. 3-T imaging of the cranial nerves using three-dimensional reversed FISP with diffusion-weighted MR sequence. *J Magn Reson Imaging*. 2008;27(3):454–8.
9. Chhabra A, Bajaj G, Wadhwa V, Quadri RS, White J, Myers LL, et al. MR Neurographic Evaluation of Facial and Neck Pain: Normal and Abnormal Craniospinal Nerves below the Skull Base. *RadioGraphics*. 2018;38(5):1498–513.
10. Klupp E, Cervantes B, Sollmann N, Treibel F, Weidlich D, Baum T, et al. Improved Brachial Plexus Visualization Using an Adiabatic iMSDE-Prepared STIR 3D TSE. *Clin Neuroradiol*. 2019;29(4):631–8.
11. Yoneyama M, Takahara T, Kwee TC, Nakamura M, Tabuchi T. Rapid high resolution MR neurography with a diffusion-weighted pre-pulse. *Magn Reson Med Sci [Internet]*. 2013;12(2):111–9. Available from: <http://www.ncbi.nlm.nih.gov/pubmed/23666153>
12. Saito S, Ozawa H, Fujioka M, Hikishima K, Hata J, Kurihara S, et al. Visualization of nerve fibers around the carotid bifurcation with use of a 9.4 Tesla microscopic magnetic resonance diffusion tensor imaging with tractography. *Head Neck*. 2018;40(10):2228–34.
13. Jacquesson T, Frindel C, Kocovar G, Berhouma M, Jouanneau E, Attyé A, et al. Overcoming Challenges of Cranial Nerve Tractography: A Targeted Review. *Clin Neurosurg*. 2019;84(2):313–25.
14. Burian E, Probst FA, Cornelius C. MRI of the inferior alveolar nerve and lingual nerve – anatomical variation and morphometric benchmark values of nerve diameters in healthy subjects. *Clin Oral Investig*. 2019;
15. Dalrymple NC, Prasad SR, Freckleton MW, Chintapalli KN. Informatics in radiology

(infoRAD): Introduction to the language of three-dimensional imaging with multidetector CT. *Radiographics*. 2005;25(5):1409–28.

16. Napel S, Rubin GD, Jeffrey RB. Sts-mip: A new reconstruction technique for ct of the chest. *J Comput Assist Tomogr*. 1993;
17. Joo W, Yoshioka F, Funaki T, Mizokami K, Rhoton AL. Microsurgical anatomy of the trigeminal nerve. *Clin Anat*. 2014;27(1):61–88.
18. Woolfall P, Coulthard a. Pictorial review: Trigeminal nerve: anatomy and pathology. *Br J Radiol*. 2001;74(881):458–67.
19. Bathla G, Hegde AN. The trigeminal nerve: An illustrated review of its imaging anatomy and pathology. *Clin Radiol [Internet]*. 2013;68(2):203–13. Available from: <http://dx.doi.org/10.1016/j.crad.2012.05.019>
20. Bathla G, Hegde AN. The trigeminal nerve: An illustrated review of its imaging anatomy and pathology. *Clin Radiol [Internet]*. 2013;68(2):203–13. Available from: <http://dx.doi.org/10.1016/j.crad.2012.05.019>
21. Dessouky R, Xi Y, Zuniga J, Chhabra A. Role of MR Neurography for the Diagnosis of Peripheral Trigeminal Nerve Injuries in Patients with Prior Molar Tooth Extraction. *Am J Neuroradiol*. 2018;39(1):162–9.
22. Van der Cruyssen F, Peeters F, Croonenborghs T-M, Fransen J, Renton T, Politis C, et al. A systematic review on diagnostic test accuracy of magnetic resonance neurography versus clinical neurosensory assessment for post-traumatic trigeminal neuropathy in patients reporting neurosensory disturbance. *Dentomaxillofacial Radiol [Internet]*. 2020 May 27;(March):20200103. Available from: <https://www.birpublications.org/doi/10.1259/dmfr.20200103>
23. Hwang L, Dessouky R, Xi Y, Amirlak B, Chhabra A. MR neurography of greater occipital nerve neuropathy: Initial experience in patients with migraine. *Am J Neuroradiol*. 2017;38(11):2203–9.
24. Gupta S, Mendis F, Hagiwara M, Fatterpekar G, Roehm PC. Imaging the Facial Nerve: A Contemporary Review. *Radiol Res Pract*. 2013;2013:1–14.
25. Myckatyn TM, Mackinnon SE. A Review of Facial Nerve Anatomy. *Semin Plast Surg*. 2004;18(1):5–11.
26. Casselman JW, Kuhweide R, Deimling M, Ampe W, Dehaene I, Meeus L. Constructive interference in steady state-3DFT MR imaging of the inner ear and cerebellopontine angle. *Am J Neuroradiol*. 1993;14(1):47–57.
27. Meng Q, Guan J, Rao L, Chu J, Li S, Zhou Z, et al. High-Resolution MRI of the Intraparotid Facial Nerve Based on a Microsurface Coil and a 3D Reversed Fast Imaging with Steady-State Precession DWI Sequence at 3T. *Am J Neuroradiol*. 2013;34(8):1643–8.
28. Wen J, Desai NS, Jeffery D, Aygun N, Blitz A. High-Resolution Isotropic Three-Dimensional MR Imaging of the Extraforaminal Segments of the Cranial Nerves. *Magn Reson Imaging Clin N Am [Internet]*. 2018;26(1):101–19. Available from: <https://doi.org/10.1016/j.mric.2017.08.007>
29. Fujii H, Fujita A, Yang A, Kanazawa H, Buch K, Sakai O, et al. Visualization of the Peripheral Branches of the Mandibular Division of the Trigeminal Nerve on 3D Double-Echo Steady-State with Water Excitation Sequence. *Am J Neuroradiol [Internet]*. 2015 Jul;36(7):1333–7. Available from: <http://www.embase.com/search/results?subaction=viewrecord&from=export&id=L605294837>

- 1 30. Fuji H. Localization of Parotid Gland Tumors in Relation to the Intraparotid Facial
2 Nerve on 3D Double-Echo Steady-State with Water Excitation Sequence. 2019;1–6.
- 3 31. Santos JMG, Jiménez SS, Pérez MT, Cascales MM, Marty JL, Marín MAF-V. Tracking the
4 glossopharyngeal nerve pathway through anatomical references in cross-sectional
5 imaging techniques: a pictorial review. *Insights Imaging*. 2018;9(4):559–69.
- 6 32. Sakamoto Y. Morphological Features of the Branching Pattern of the Hypoglossal
7 Nerve. *Anat Rec*. 2019;302(4):558–67.
- 8 33. Yuan H, Silberstein SD. Vagus Nerve and Vagus Nerve Stimulation, a Comprehensive
9 Review: Part I. Headache *J Head Face Pain*. 2016;56(1):71–8.
- 10 34. Tubbs RS, Mortazavi MM, Loukas M, D’Antoni A V., Shoja MM, Chern JJ, et al.
11 Anatomical study of the third occipital nerve and its potential role in occipital
12 headache/neck pain following midline dissections of the craniocervical junction:
13 Laboratory investigation. *J Neurosurg Spine*. 2011;15(1):71–5.
- 14 35. Durazzo MD, Furlan JC, Teixeira G V., Friguglietti CUM, Kulcsar MAV, Magalhaes RP, et
15 al. Anatomic landmarks for localization of the spinal accessory nerve. *Clin Anat*.
16 2009;22(4):471–5.
- 17 36. Johal J, Iwanaga J, Tubbs K, Loukas M, Oskouian RJ, Tubbs RS. The Accessory Nerve: A
18 Comprehensive Review of its Anatomy, Development, Variations, Landmarks and
19 Clinical Considerations. *Anat Rec (Hoboken)*. 2018;302(4):620–9.
- 20 37. Overland J, Hodge JC, Breik O, Krishnan S. Surgical anatomy of the spinal accessory
21 nerve: Review of the literature and case report of a rare anatomical variant. *J Laryngol*
22 *Otol*. 2016;130(10):969–72.
- 23 38. Kim DDD, Caccamese JFF, Ord RAA. Variations in the course of the hypoglossal nerve:
24 a case report and literature review. *Int J Oral Maxillofac Surg [Internet]*.
25 2003;32(5):568–70. Available from: [http://dx.doi.org/10.1016/S0901-5027\(02\)90360-](http://dx.doi.org/10.1016/S0901-5027(02)90360-2)
26 [2](http://dx.doi.org/10.1016/S0901-5027(02)90360-2)
- 27 39. Lin HC, Barkhaus PE. Cranial nerve XII: The hypoglossal nerve. *Semin Neurol*.
28 2009;29(1):45–52.
- 29 40. Linn J, Peters F, Moriggl B, Naidich TP, Brückmann H, Yousry I. The jugular foramen:
30 Imaging strategy and detailed anatomy at 3T. *Am J Neuroradiol*. 2009;30(1):34–41.
- 31 41. Bovim G, Bonamico L, Frederiksen TA, Lindboe CF, Stolt-Nielsen A, Sjaastad O.
32 Topographic Variations in the Peripheral Course of the Greater Occipital Nerve. *Spine*
33 (Phila Pa 1976) [Internet]. 1991 Apr;16(4):475–8. Available from:
34 <https://insights.ovid.com/crossref?an=00007632-199104000-00017>
- 35 42. Mosser SW, Guyuron B, Janis JE, Rohrich RJ. The anatomy of the greater occipital
36 nerve: Implications for the etiology of migraine headaches. *Plast Reconstr Surg*.
37 2004;113(2):693–7.
- 38 43. Kwon HJ, Kim HS, Jehoon O, Kang HJ, Won JY, Yang HM, et al. Anatomical analysis of
39 the distribution patterns of occipital cutaneous nerves and the clinical implications for
40 pain management. *J Pain Res*. 2018;11:2023–31.
- 41 44. Cohen-Gadol A, Kemp III W, Tubbs Rs. The innervation of the scalp: A comprehensive
42 review including anatomy, pathology, and neurosurgical correlates. *Surg Neurol Int*.
43 2011;2(1):178.
- 44 45. Lee M, Brown M, Chepla K, Okada H, Gatherwright J, Totonchi A, et al. An anatomical
45 study of the lesser occipital nerve and its potential compression points: Implications
46 for surgical treatment of migraine headaches. *Plast Reconstr Surg*. 2013;132(6):1551–
47 6.

- 1 46. Voskuilen L, de Heer P, van der Molen L, Balm AJM, van der Heijden F, Strijkers GJ, et al. A 12-channel flexible receiver coil for accelerated tongue imaging. *Magn Reson Mater Physics, Biol Med* [Internet]. 2020;(0123456789). Available from: <https://doi.org/10.1007/s10334-019-00824-5>
- 2
- 3
- 4
- 5 47. Wessig C, Bendszus M, Stoll G. In vivo visualization of focal demyelination in peripheral nerves by gadofluorine M-enhanced magnetic resonance imaging. *Exp Neurol*. 2007;204(1):14–9.
- 6
- 7
- 8
- 9 48. Zuniga JR, Mistry C, Tikhonov I, Dessouky R, Chhabra A, Zuniga JR, et al. Magnetic Resonance Neurography of Traumatic and Nontraumatic Peripheral Trigeminal Neuropathies. *J ORAL Maxillofac Surg*. 2018;76(4):725–36.
- 10
- 11
- 12
- 13 49. Takagi T, Nakamura M, Yamada M, Hikishima K, Momoshima S, Fujiyoshi K, et al. Visualization of peripheral nerve degeneration and regeneration: Monitoring with diffusion tensor tractography. *Neuroimage* [Internet]. 2009;44(3):884–92. Available from: <http://dx.doi.org/10.1016/j.neuroimage.2008.09.022>
- 14
- 15
- 16
- 17
- 18 50. Kininy W El, Roddy D, Davy S, Roman E, O’Keefe V, O’Hanlon E, et al. Magnetic resonance diffusion weighted imaging using constrained spherical deconvolution-based tractography of the extracranial course of the facial nerve. *Oral Surg Oral Med Oral Pathol Oral Radiol* [Internet]. 2020;00(00):1–13. Available from: <https://doi.org/10.1016/j.oooo.2019.12.012>
- 19
- 20
- 21
- 22
- 23 51. Rouchy R-C, Attyé A, Medici M, Renard F, Kastler A, Grand S, et al. Facial nerve tractography: A new tool for the detection of perineural spread in parotid cancers. *Eur Radiol*. 2018;28(9):3861–71.
- 24
- 25
- 26
- 27
- 28 52. Xie G, Zhang F, Leung L, Mooney MA, Epprecht L, Norton I, et al. Anatomical assessment of trigeminal nerve tractography using diffusion MRI: A comparison of acquisition b-values and single- and multi-fiber tracking strategies. *NeuroImage Clin* [Internet]. 2020;25(September 2019):102160. Available from: <https://doi.org/10.1016/j.nicl.2019.102160>
- 29
- 30
- 31
- 32
- 33 53. Terumitsu M, Matsuzawa H, Seo K, Watanabe M, Kurata S, Suda A, et al. High-contrast high-resolution imaging of posttraumatic mandibular nerve by 3DAC-PROPELLER magnetic resonance imaging: correlation with the severity of sensory disturbance. *Oral Surg Oral Med Oral Pathol Oral Radiol* [Internet]. 2017 Jul;124(1):85–94. Available from: <https://www.ncbi.nlm.nih.gov/pubmed/28499808>
- 34
- 35
- 36
- 37
- 38 54. Shapey J, Vos SB, Vercauteren T, Bradford R, Saeed SR, Bisdas S, et al. Clinical applications for diffusion MRI and tractography of cranial nerves within the posterior fossa: A systematic review. *Front Neurosci*. 2019;13(FEB).
- 39
- 40
- 41
- 42 55. Cauley KA, Filippi CG. Diffusion-tensor imaging of small nerve bundles: Cranial nerves, peripheral nerves, distal spinal cord, and lumbar nerve roots- Clinical applications. *Am J Roentgenol*. 2013;201(2):326–35.
- 43
- 44
- 45
- 46
- 47 56. Manoliu A, Ho M, Nanz D, Dappa E, Boss A, Grodzki DM, et al. MR neurographic orthopantomogram: Ultrashort echo-time imaging of mandibular bone and teeth complemented with high-resolution morphological and functional MR neurography. *J Magn Reson Imaging*. 2016;44(2):393–400.
- 48
- 49
- 50
- 51 57. Zhu B, Liu JZ, Cauley SF, Rosen BR, Rosen MS. Image reconstruction by domain-transform manifold learning. *Nature*. 2018;555(7697):487–92.
- 52
- 53
- 54
- 55 58. Lundervold AS, Lundervold A. An overview of deep learning in medical imaging focusing on MRI. *Z Med Phys* [Internet]. 2019;29(2):102–27. Available from: <https://doi.org/10.1016/j.zemedi.2018.11.002>
- 56
- 57
- 58
- 59
- 60
- 61
- 62
- 63
- 64
- 65

1
2
3
4
5
6
7
8
9
10
11
12
13
14
15
16
17
18
19
20
21
22
23
24
25
26
27
28
29
30
31
32
33
34
35
36
37
38
39
40
41
42
43
44
45
46
47
48
49
50
51
52
53
54
55
56
57
58
59
60
61
62
63
64
65

Figure captions

1 Fig 1. Coronal thick slab (5 mm) MIP/MPR images in the same subject comparing two
2 magnetic resonance neurography techniques. Short arrow: lingual nerve (V_3); long
3 arrow: inferior alveolar nerve (V_3); arrowhead: masseteric nerve (V_3). A: 3D CRANI
4 sequence. B: 3D PSIF sequence.
5
6
7

8
9 Fig 2. A: patient positioning in a standard 32 channel head coil without additional measures.
10 Note the anterior mandible is located outside the coil. B: patient positioning after
11 fixation by means of an inflatable pillow with the head in slight hyperextension using a
12 towel roll. The mandible is now well positioned within the coil. C: alternative coil,
13 being a 16 channel neck coil. D: imaging output after patient positioning as in example
14 A. Signal loss is seen at the anterior segment. E: imaging output after slight
15 hyperextension and thorough fixation as in example B. F: imaging output using a neck
16 coil after patient positioning as in example C.
17
18
19
20
21

22 Fig 3. A: orthogonal and additional planes constructed in evaluating the cranial and occipital
23 peripheral nerves. B: overall nerve anatomy discussed in this review.
24
25

26 Fig 4. A: ophthalmic division of the trigeminal nerve (V_1) using the 3D CRANI sequence. B: 3D
27 CRANI sequence. Increased caliber of the right infra-orbital nerve (V_2) in a patient with
28 SUNCT (Short lasting Unilateral Neuralgiform headache attacks with Conjunctival
29 injection and Tearing rhinorrhea and forehead sweating). C: 3D CRANI sequence.
30 Increased signal intensity is noted of the Vidian nerve (V_2) in the same patient as seen
31 in B.
32
33
34
35
36

37 Fig 5. A: anatomic relation of the anterior division of the mandibular nerve (V_3) best seen in
38 the axial plane. B: 3D CRANI sequence illustrating the buccal nerve (long arrow), the
39 masseteric nerve (short arrow) and the stem of the auriculotemporal nerve
40 (arrowhead). C: 3D CRANI sequence in a patient with post-traumatic trigeminal
41 neuropathy of the mandibular division after placement of a titanium
42 temporomandibular joint prosthesis. The left masseteric nerve is thickened and shows
43 an increased signal intensity.
44
45
46
47
48

49 Fig 6. A: anatomic overview of the posterior division of the mandibular nerve (V_3) on a
50 coronal oblique plane. B: normal appreciation of the lingual (long arrow) and inferior
51 alveolar (short arrow) nerve running between the pterygoid muscles. C: right sided
52 post-traumatic trigeminal neuropathy of the inferior alveolar nerve after ramus bone
53 grafting. D: patient with neurofibromatosis type 1, showing bilateral neurofibromas of
54 the inferior alveolar nerve at the level of the mandibular foramen.
55
56
57
58

59 Fig 7. A: anatomic overview of the facial nerve and its branches which are best seen on a
60
61
62
63
64
65

1 sagittal slightly rotated or coronal plane. B: sagittal view of a normal extracranial facial
2 nerve entering the parotid gland on a 3D CRANI thick-slab MIP/MPR-image. C: coronal
3 image with bilateral visualization of the intratemporal and extraforaminal facial nerve
4 after iatrogenic damage on the right side. A slowly recuperative facial nerve paresis
5 occurred after an infiltration with local anesthesia.
6
7

8
9 Fig. 8. A: anatomic overview of the facial (VII), hypoglossal (XII), glossopharyngeal (IX), vagus
10 (X) and accessory (XI) nerves which can be seen in close relation to each other on a coronal
11 plane. B: coronal view after a 3D CRANI sequence indicating the aforementioned peripheral
12 nerves without pathological characteristics.
13
14

15
16 Fig 9. Bilateral normal appreciation of the peripheral hypoglossal nerve (white arrows) on an
17 axial 3D CRANI image after MIP/MPR showing its course around the great vessels before
18 innervating the tongue.
19
20

21
22 Fig 10. A: anatomic overview of the occipital nerves which are seen together on an oblique
23 axial plane. B: lesser (L), third (T) and greater (G) occipital nerves after MIP/MPR on a 3D
24 CRANI sequence in a healthy subject. C: more distal course of the lesser (L) and greater (G)
25 occipital nerve in a healthy subject.
26
27

28
29 Fig 11. Panoramic curved reconstruction and MIP of the inferior alveolar nerve using a 3D
30 CRANI sequence allowing a full evaluation at a glance.
31
32

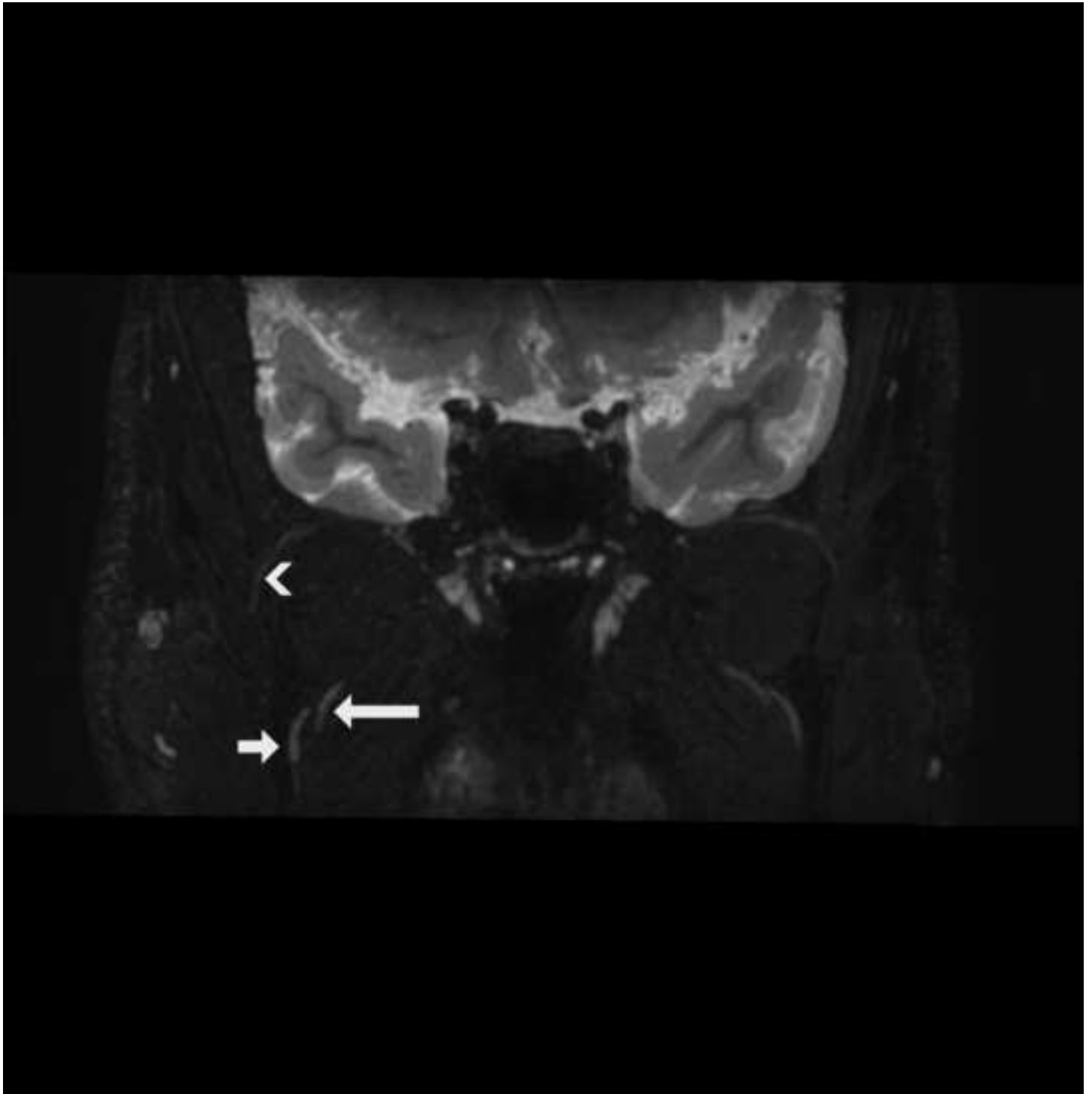
33
34 Fig 12. 3D fusion of CT and MRN images which can be valuable in planning the placement of
35 a custom made temporomandibular joint prosthesis (blue outline). The inferior alveolar
36 nerve is segmented (red outline) and indicated (white arrows) before entering the
37 mandibular canal.
38
39

40 41 **Tables**

42
43 Table 1. Magnetic resonance neurography sequences for a 3T Philips system (Philips, Best,
44 Netherlands). 3D CRANI (CRANial Nerve Imaging) and 3D PSIF (reversed fast imaging in
45 steady-state free precession) sequences. These can be further supplemented with routine
46 brain T1w, T2w, CISS and FLAIR images. TE: echo time; TR: repetition time, FOV: field-of-
47 view, STIR: short tau inversion recovery; FFE: fast field echo; N/A: not applicable; MSDE:
48 motion-sensitized driven equilibrium.
49
50
51

52 53 **Video**

54
55 Illustrative video indicating the peripheral cranial nerve anatomy using the 3D CRANI
56 sequence on a 3T Ingenia system with a 32CH head coil (Philips, Best, Netherlands).
57
58
59
60
61
62
63
64
65



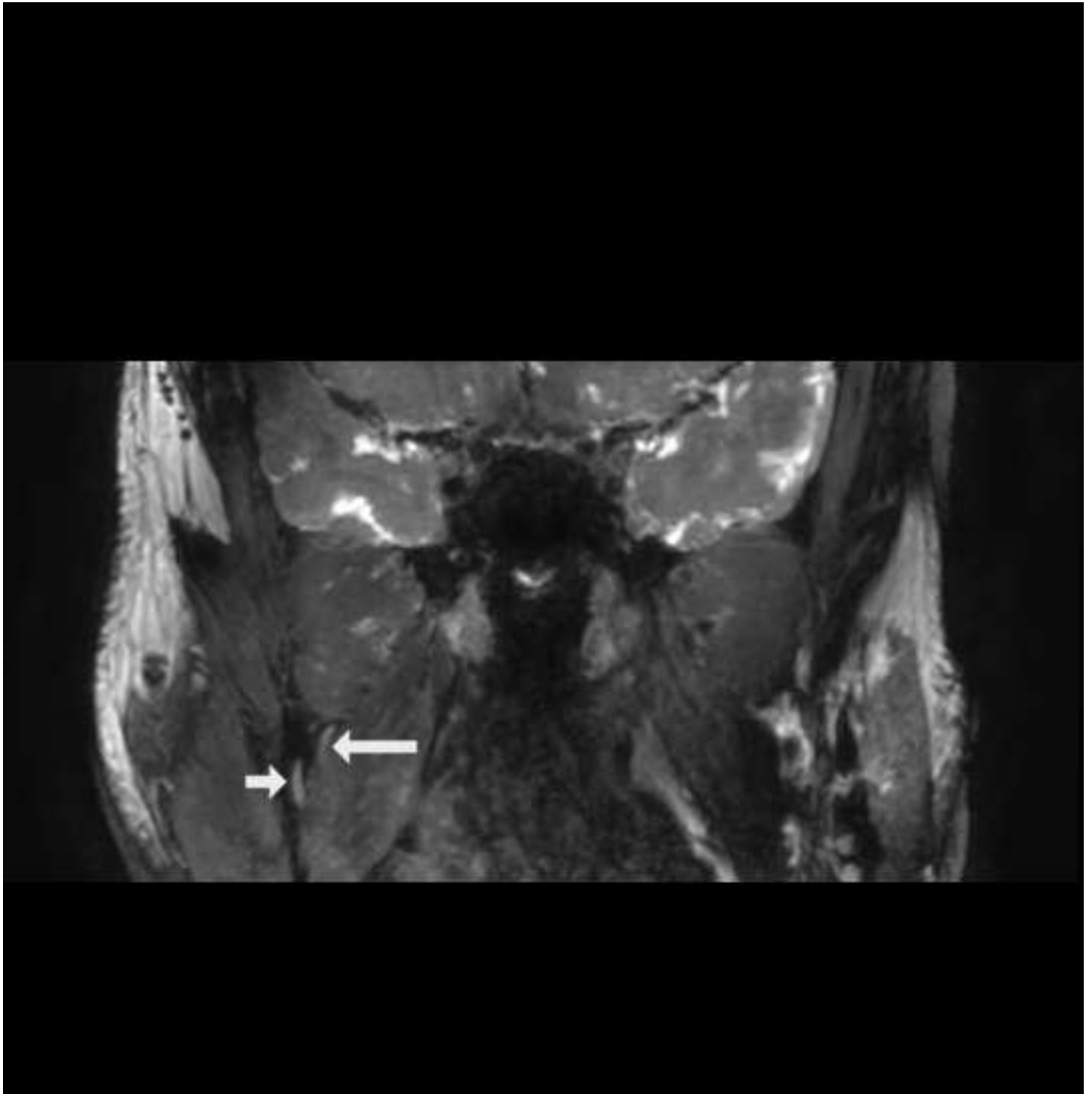


Figure 2a

[Click here to access/download;Figure;Fig 2a.tiff](#)

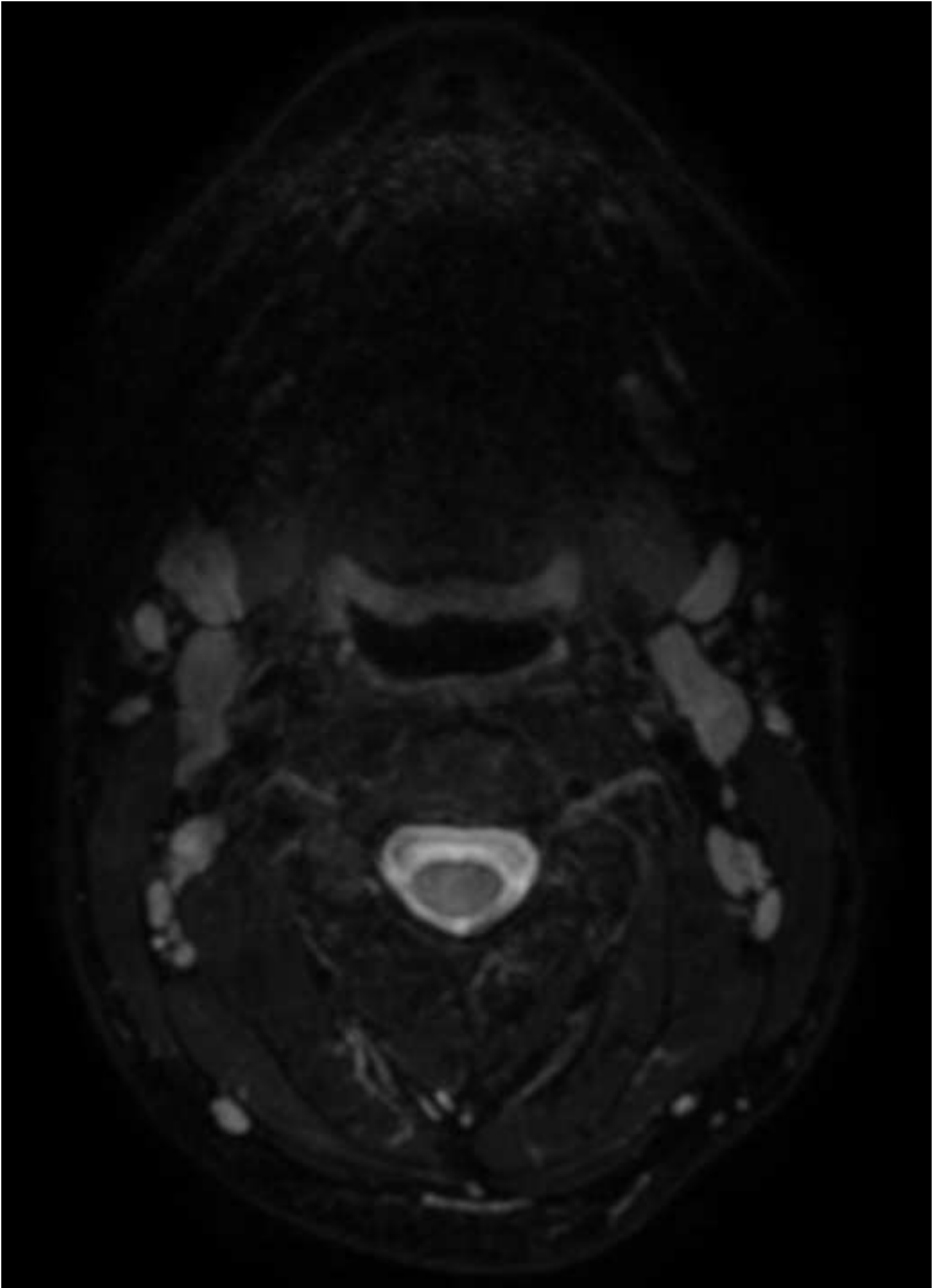


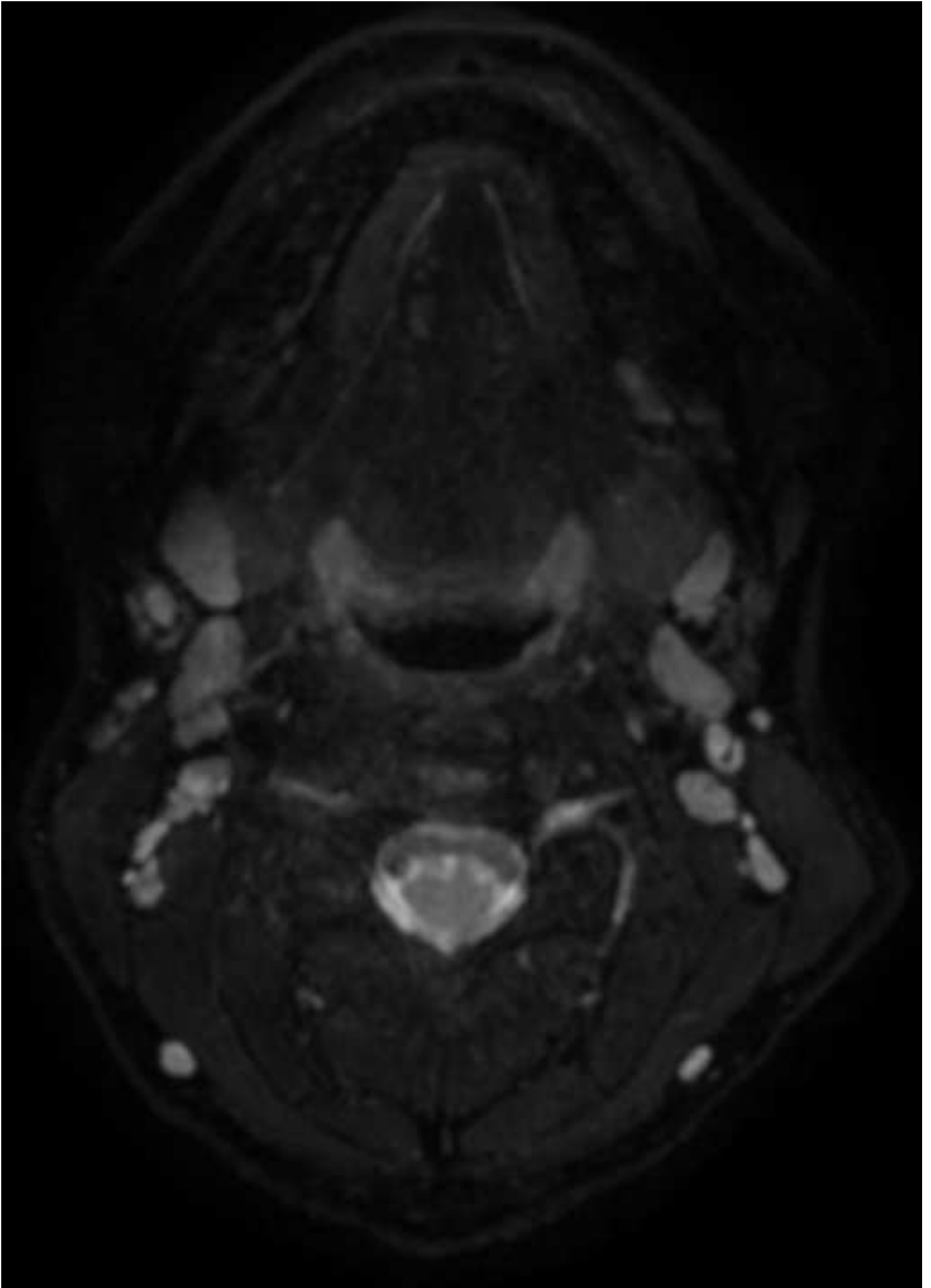


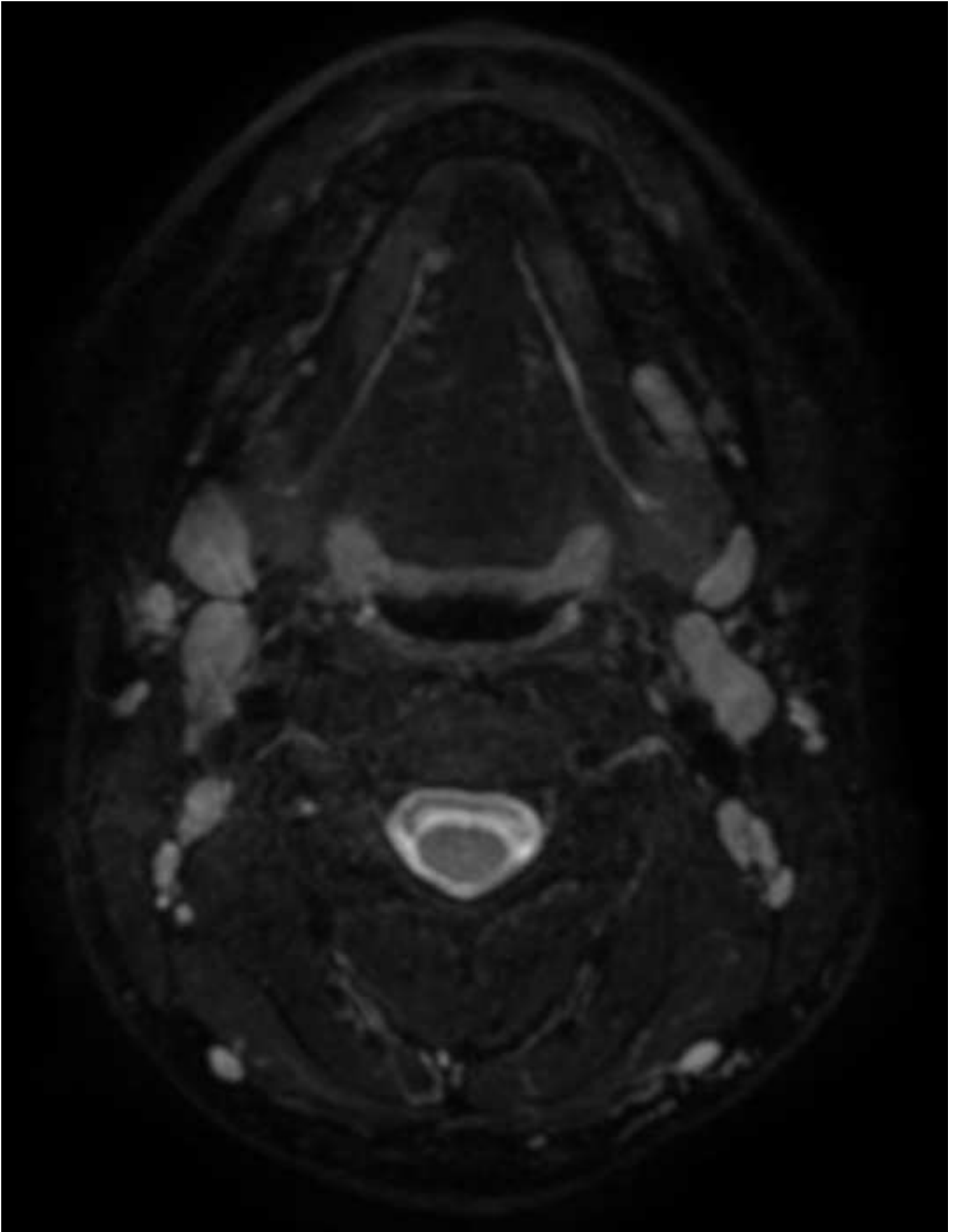
Figure 2c

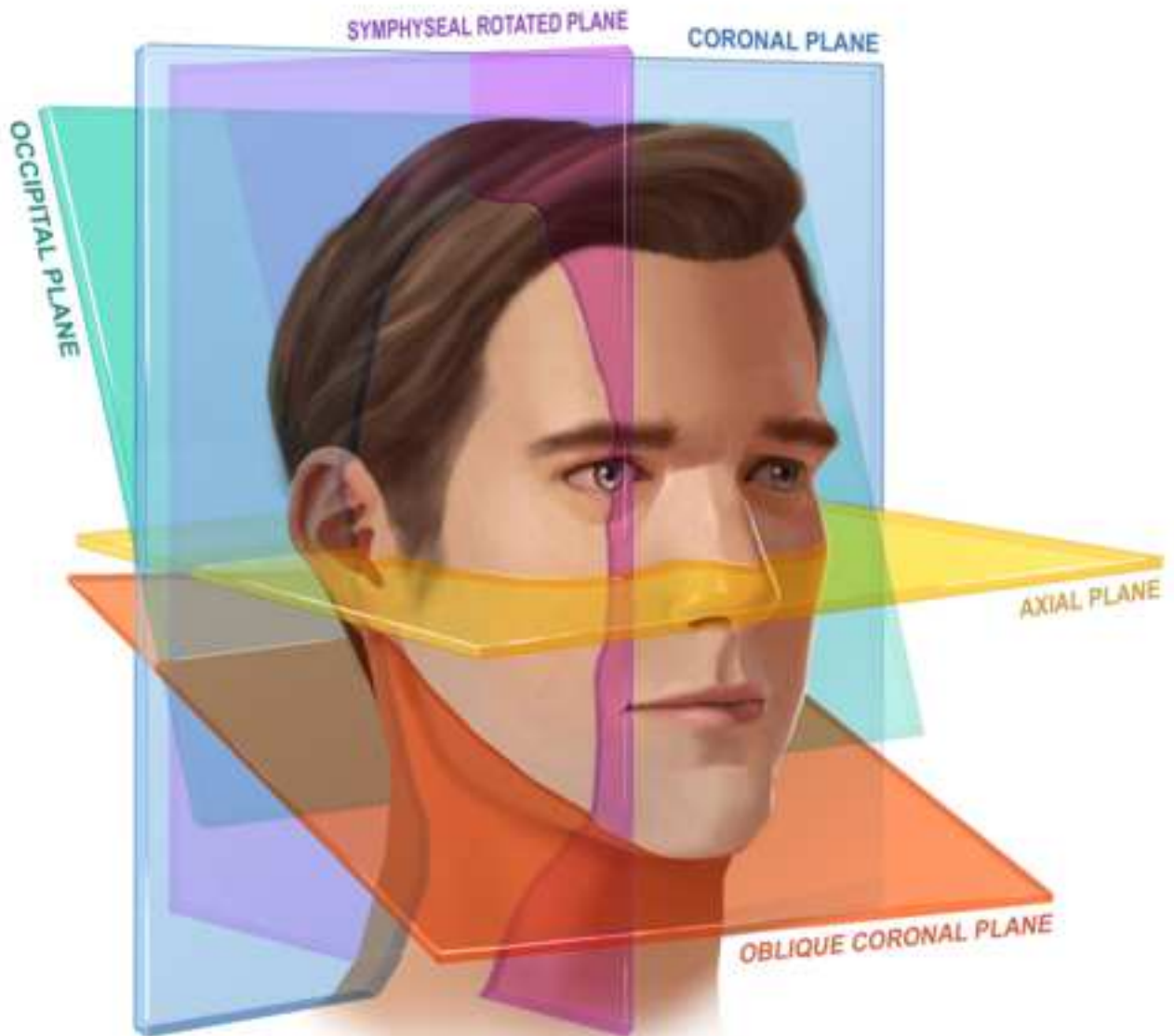
[Click here to access/download;Figure;Fig 2c.tiff](#)











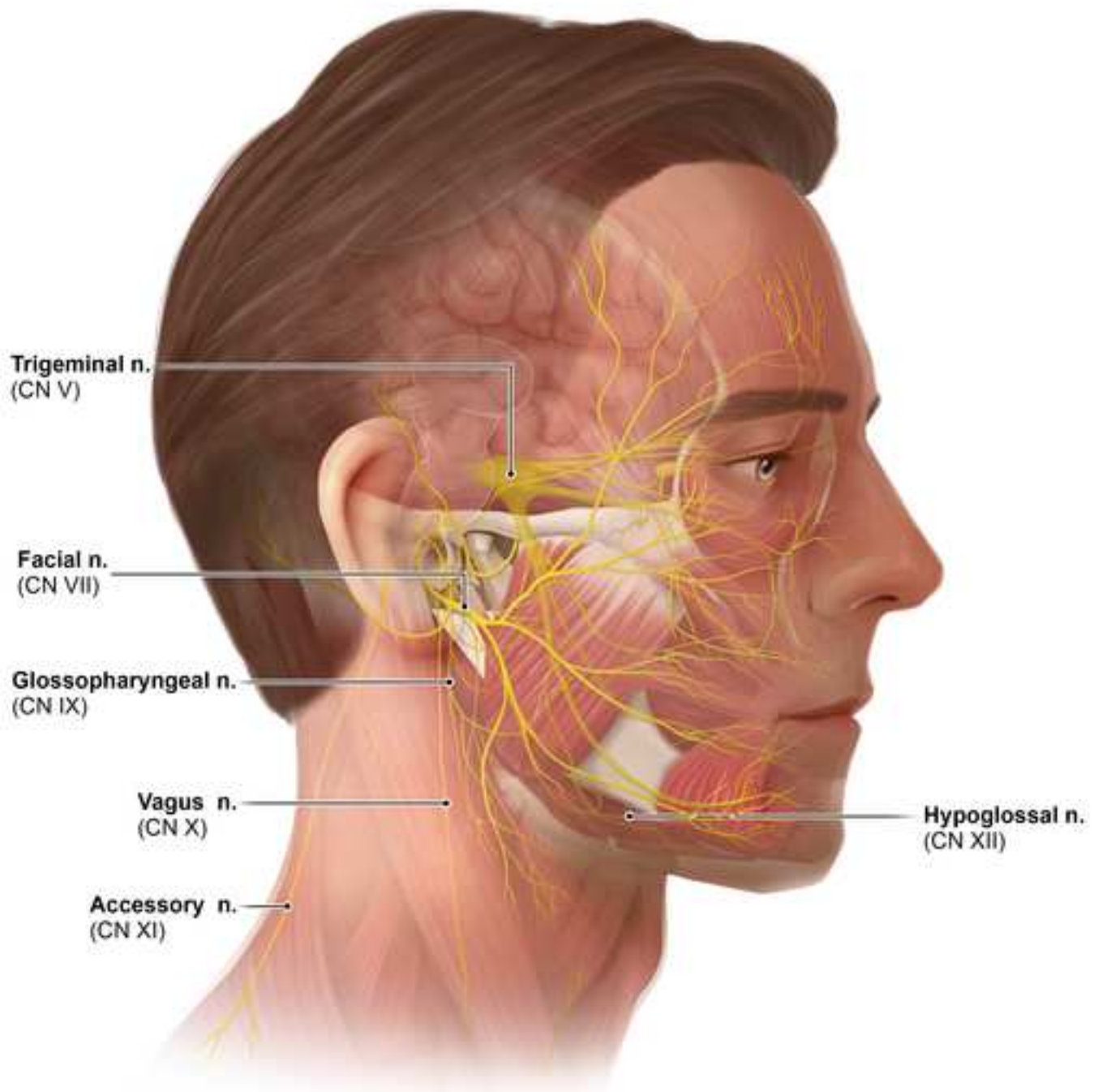
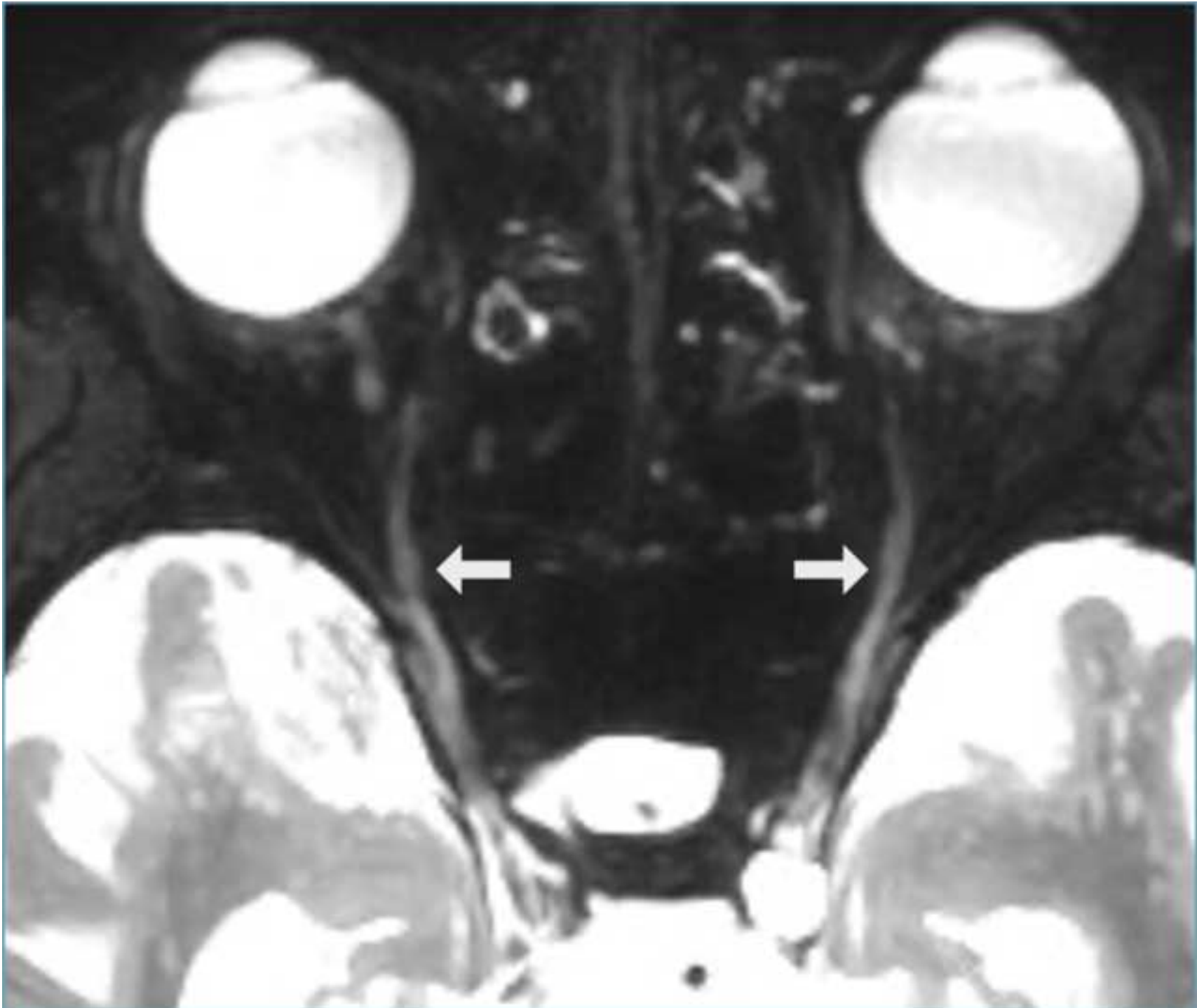
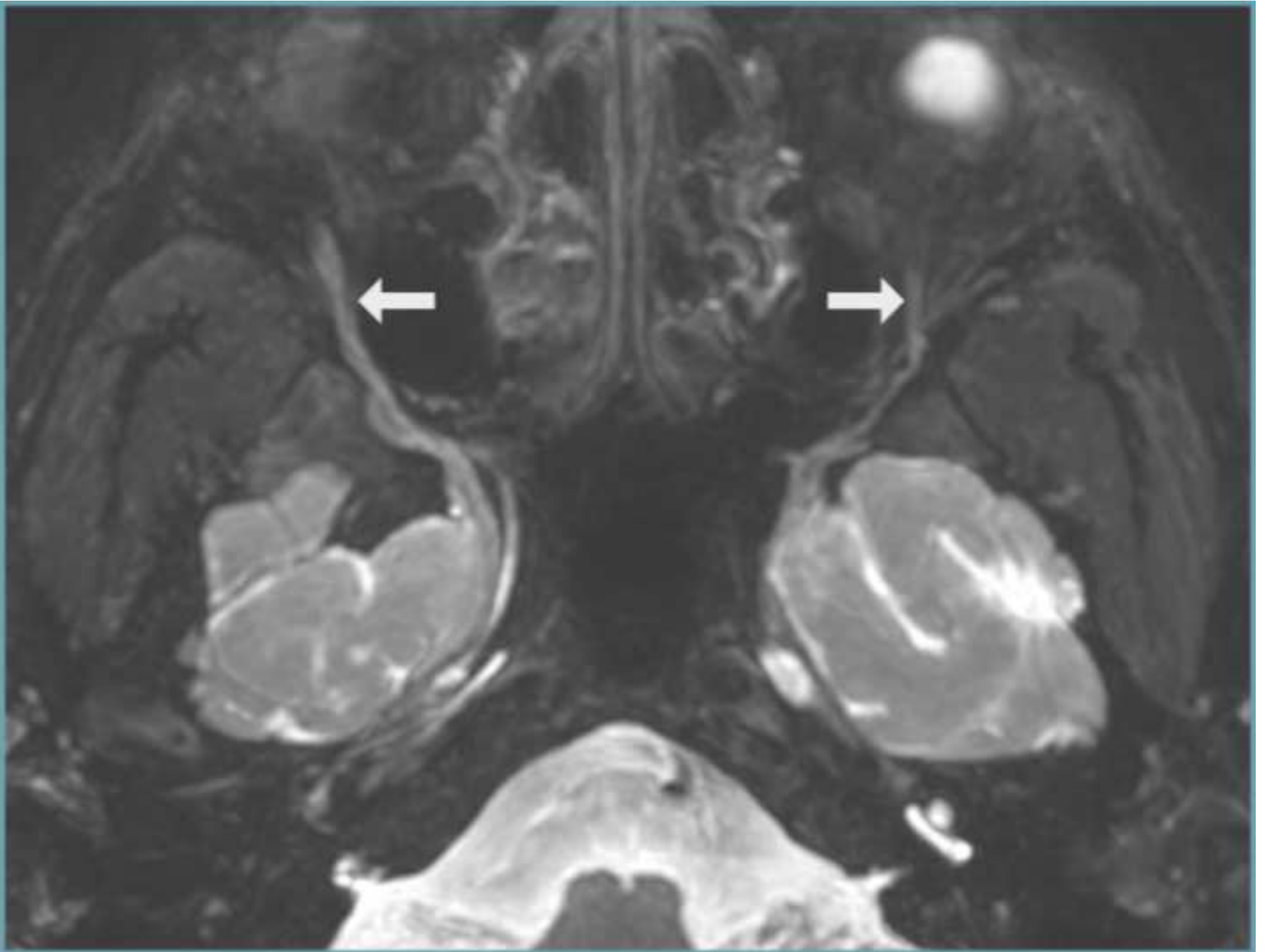
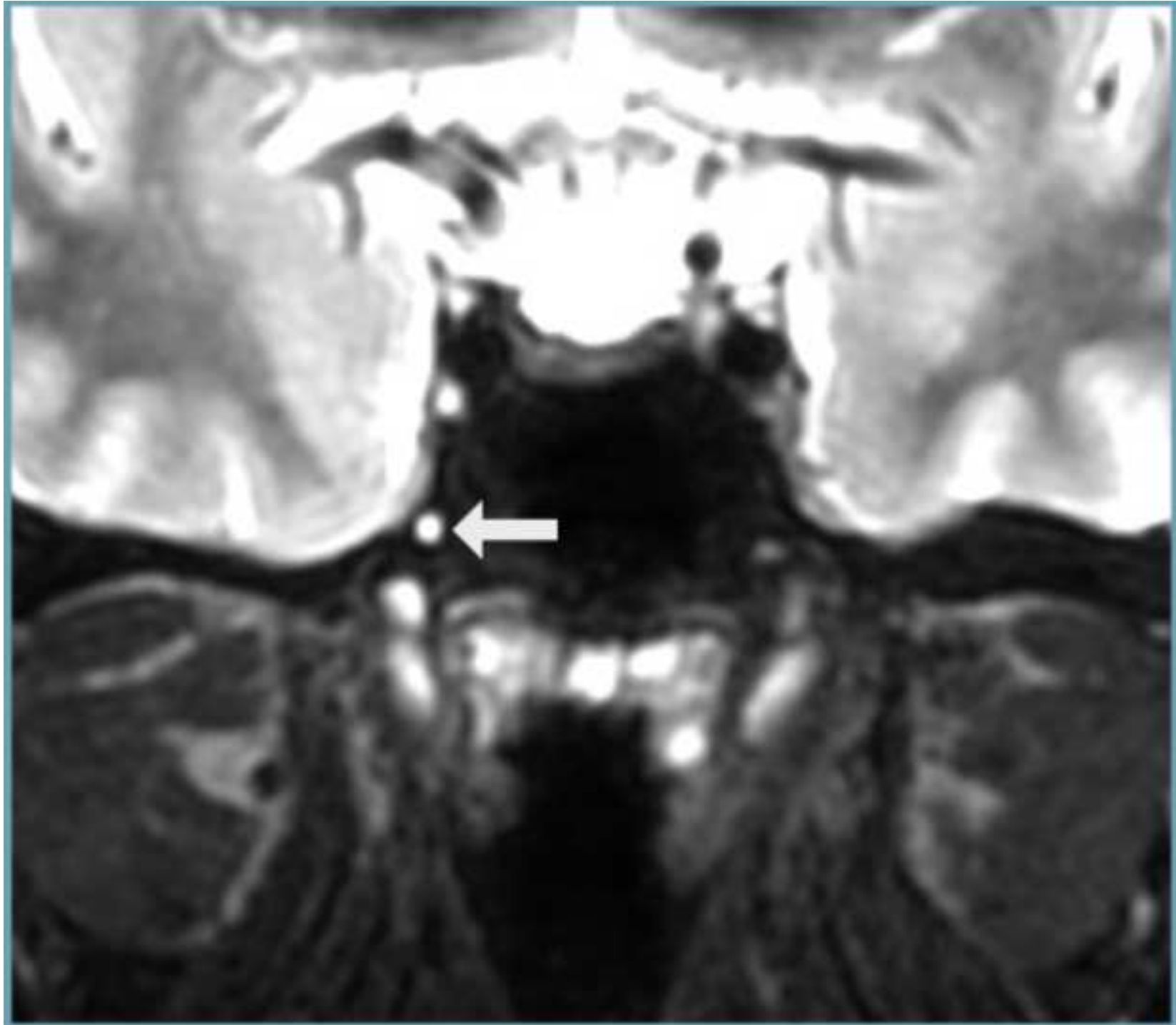
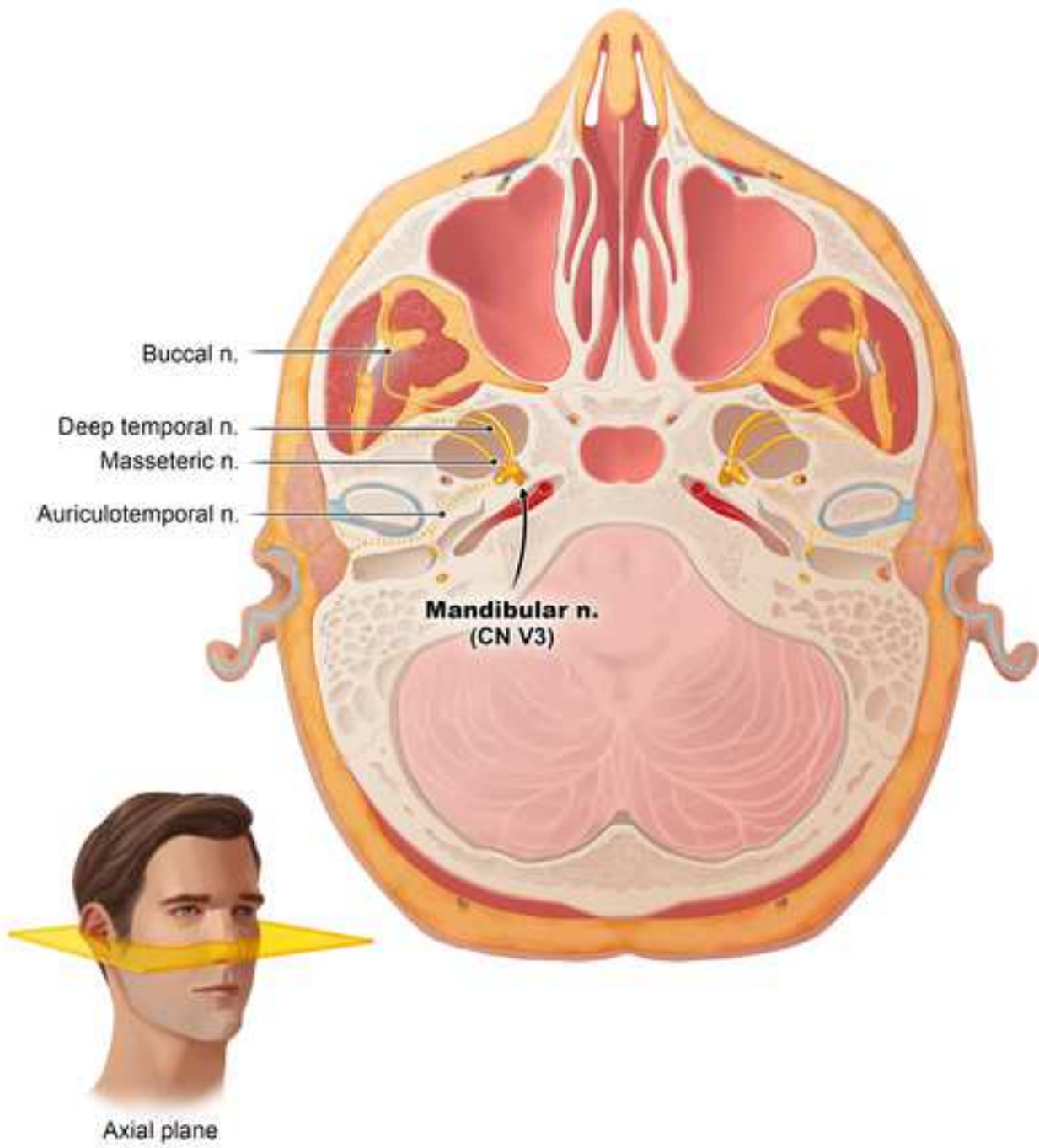


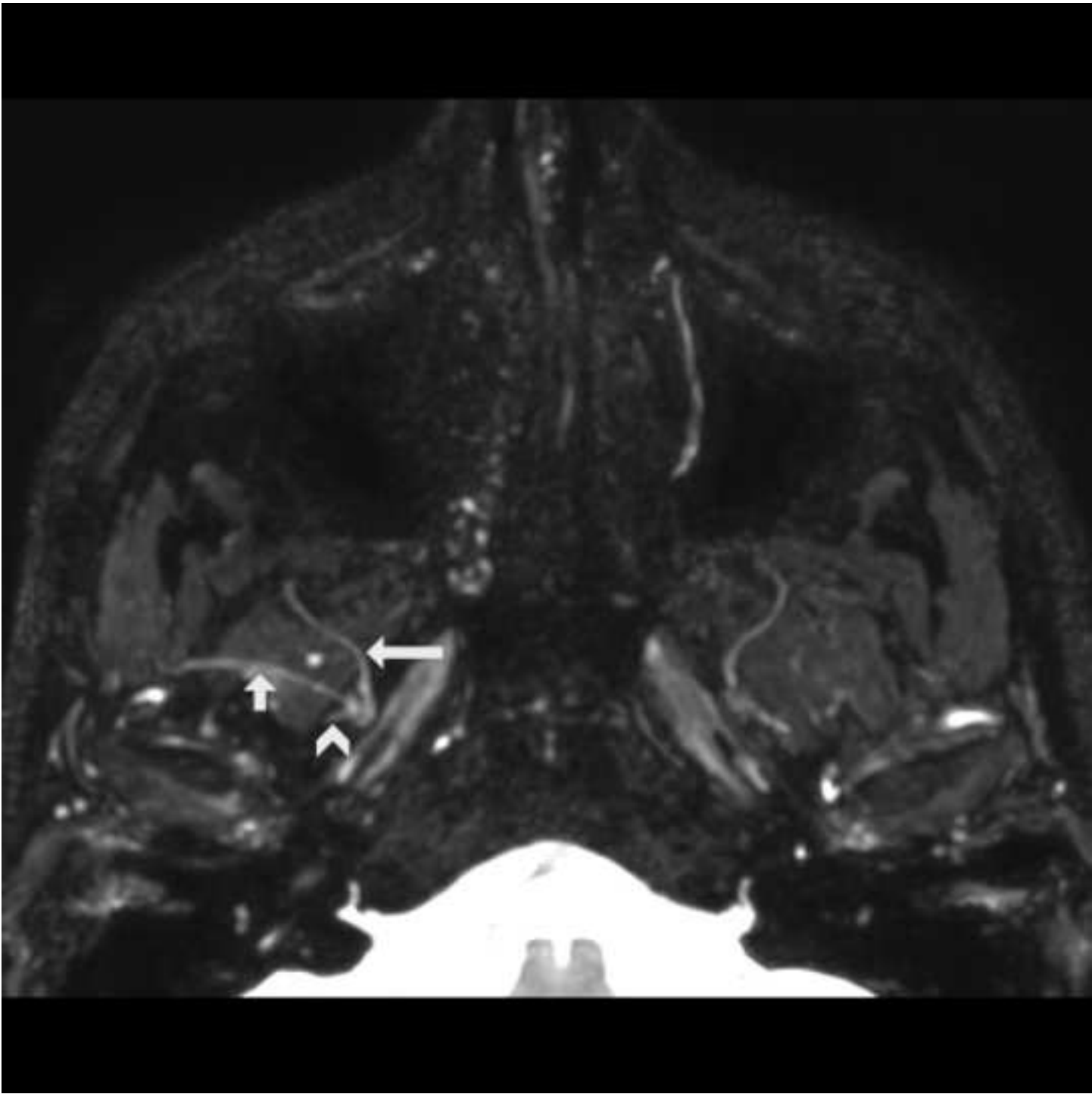
Figure 4a

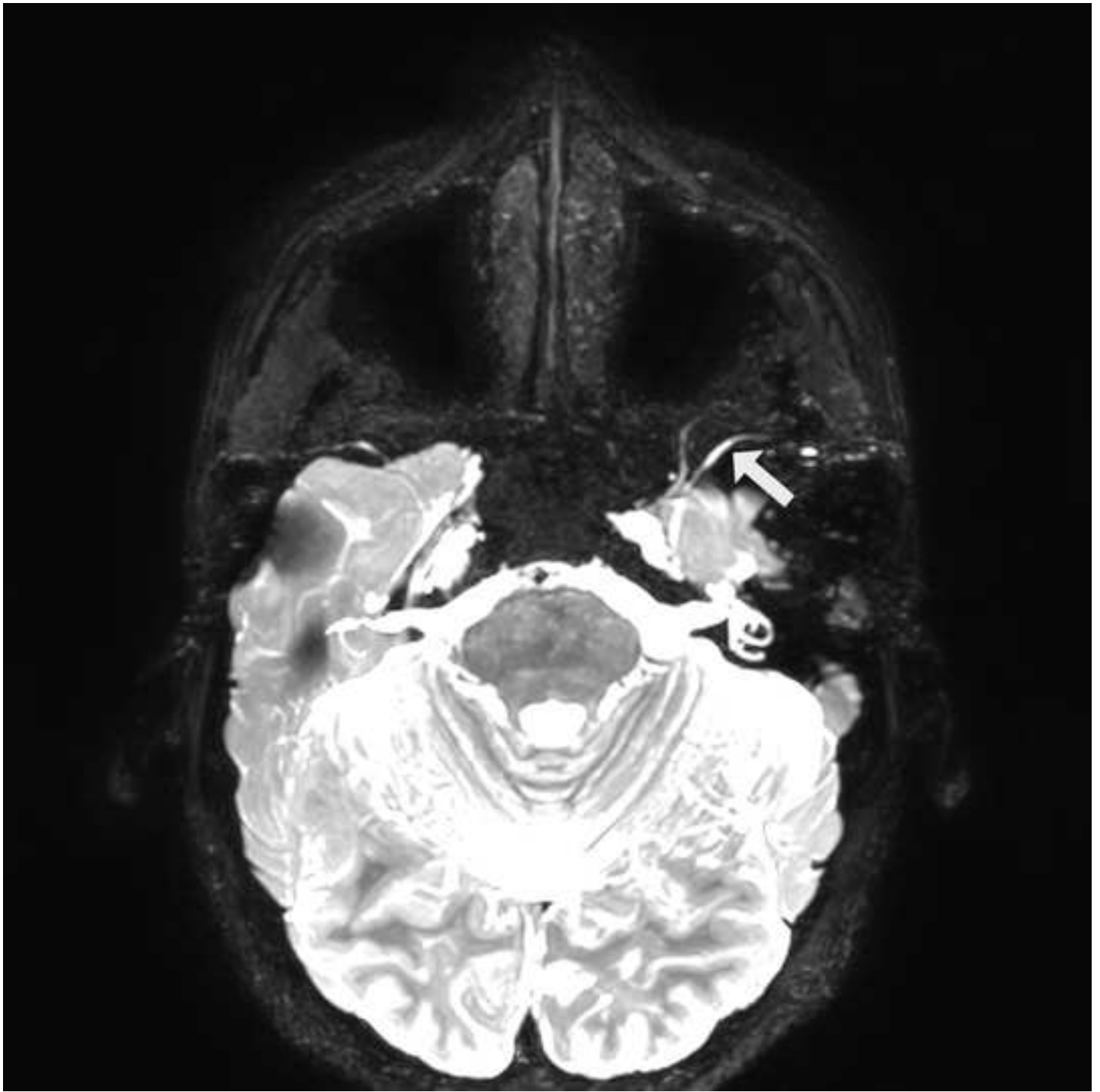


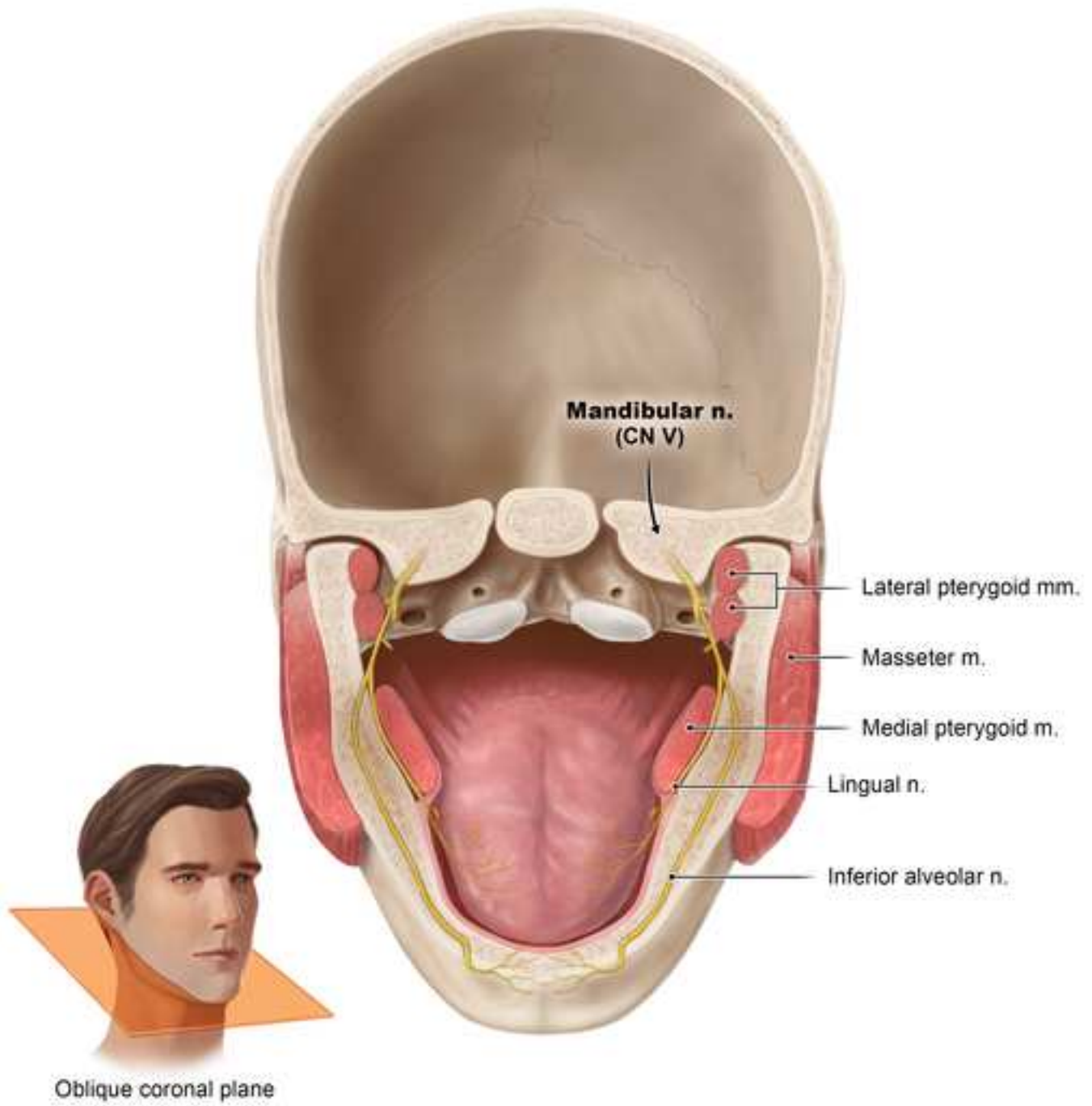


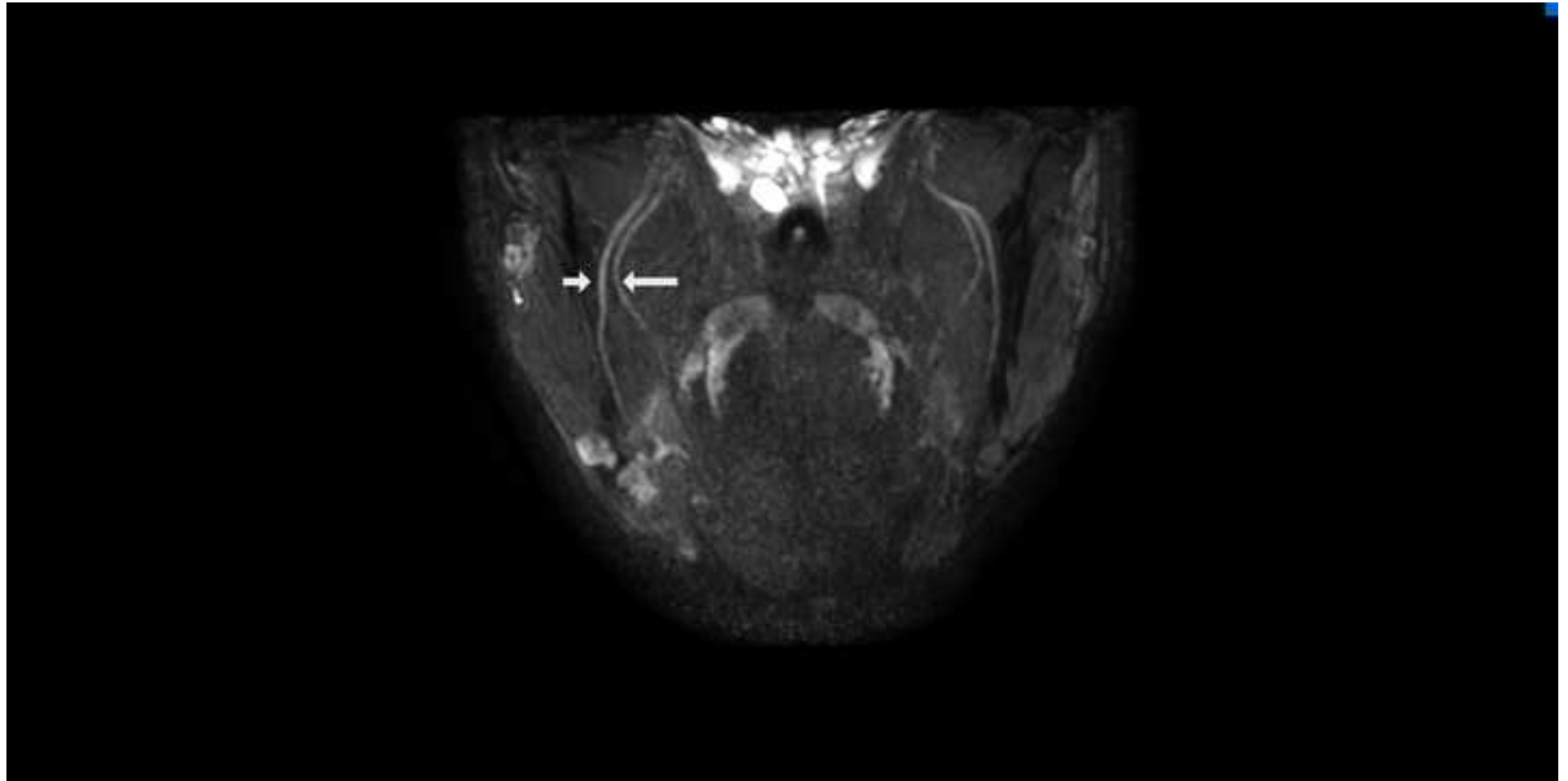


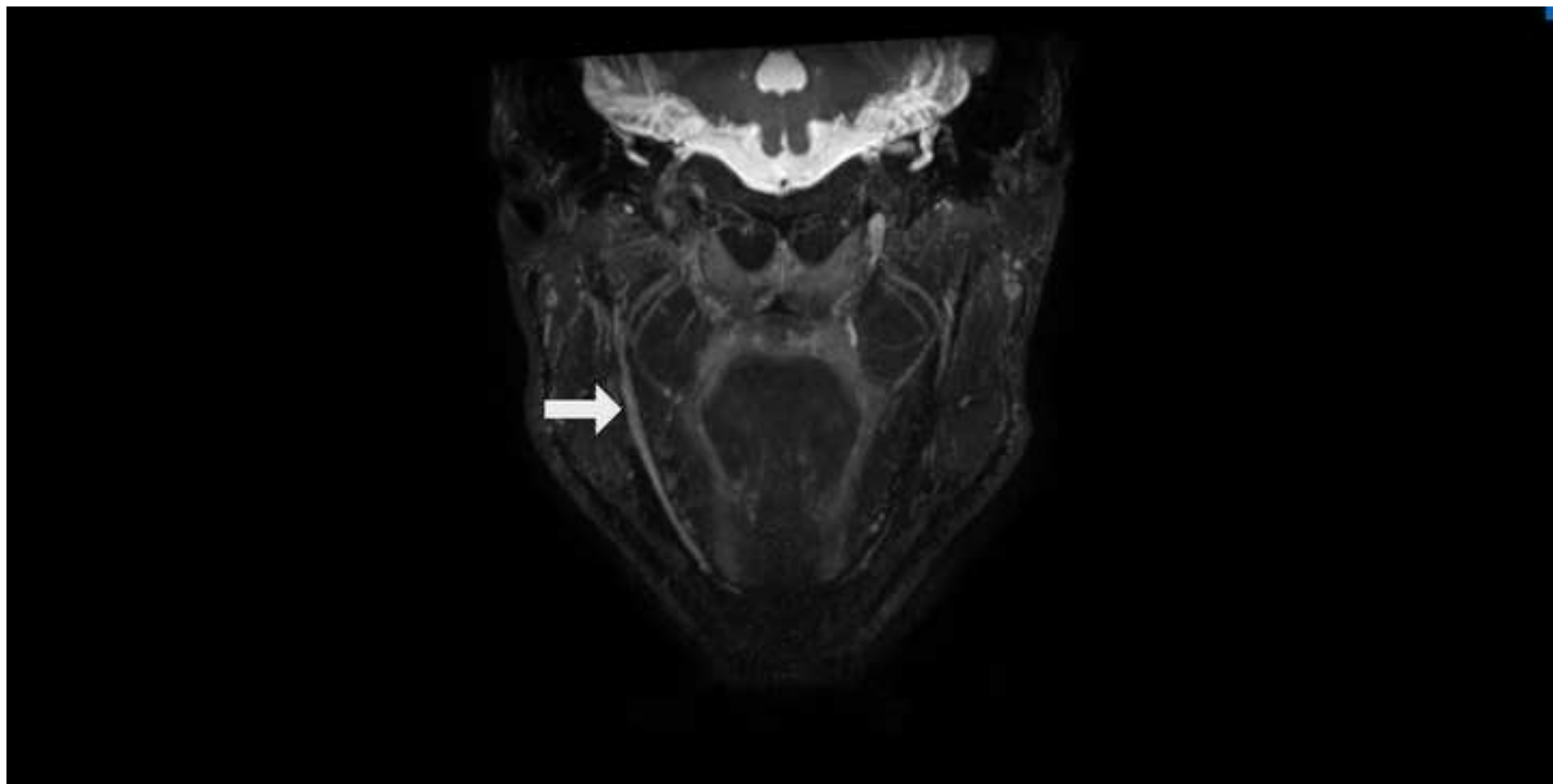




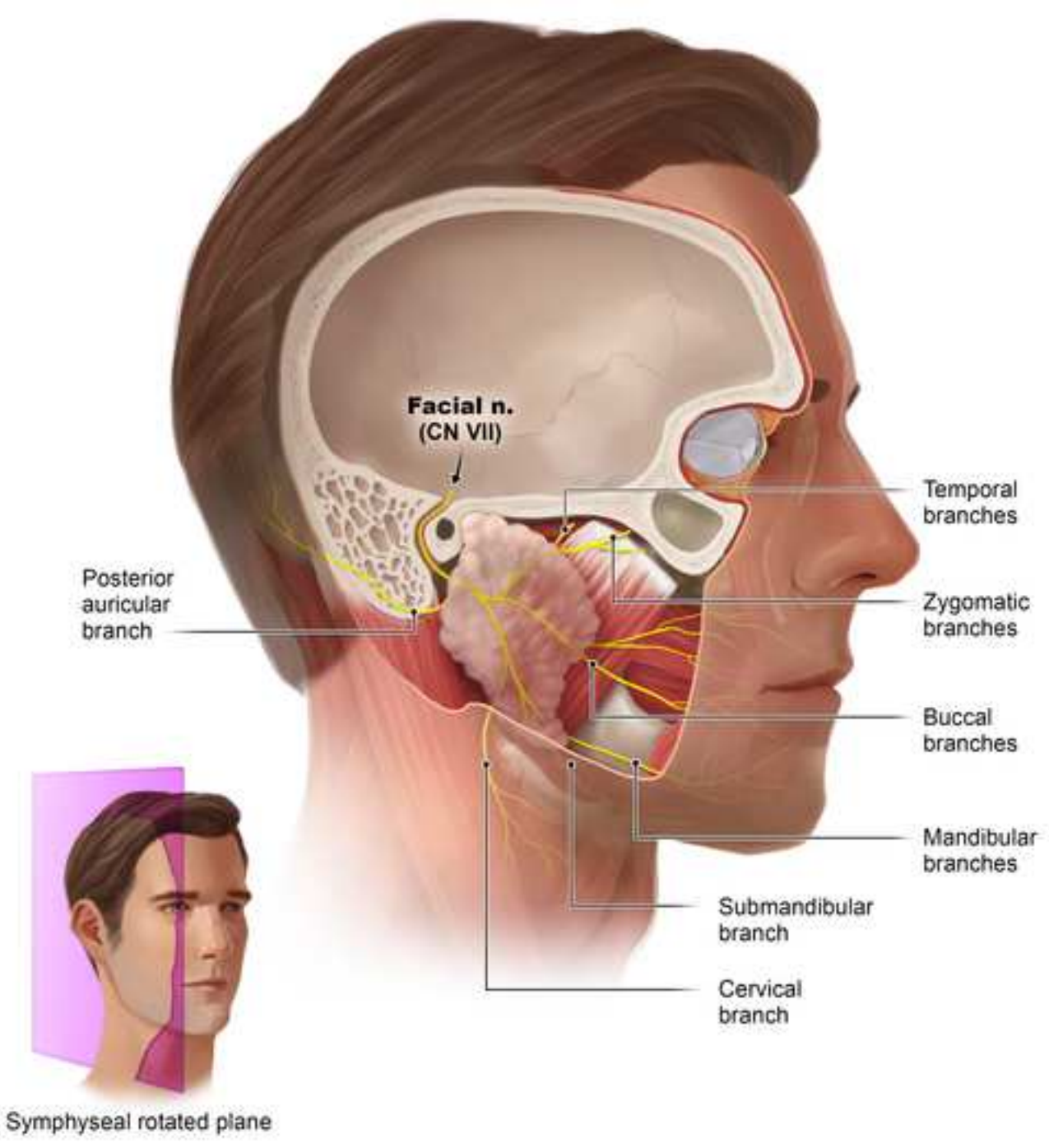


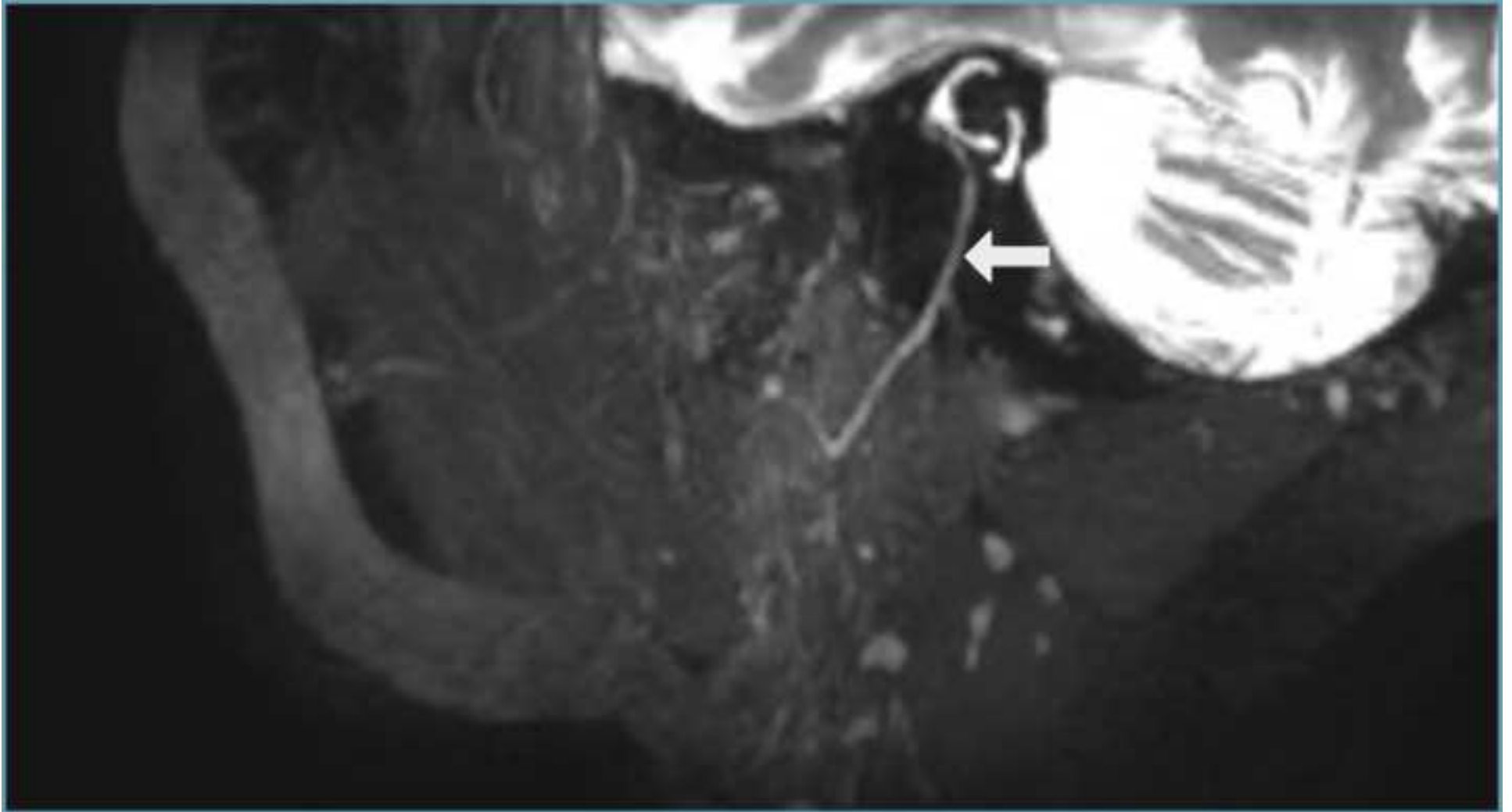


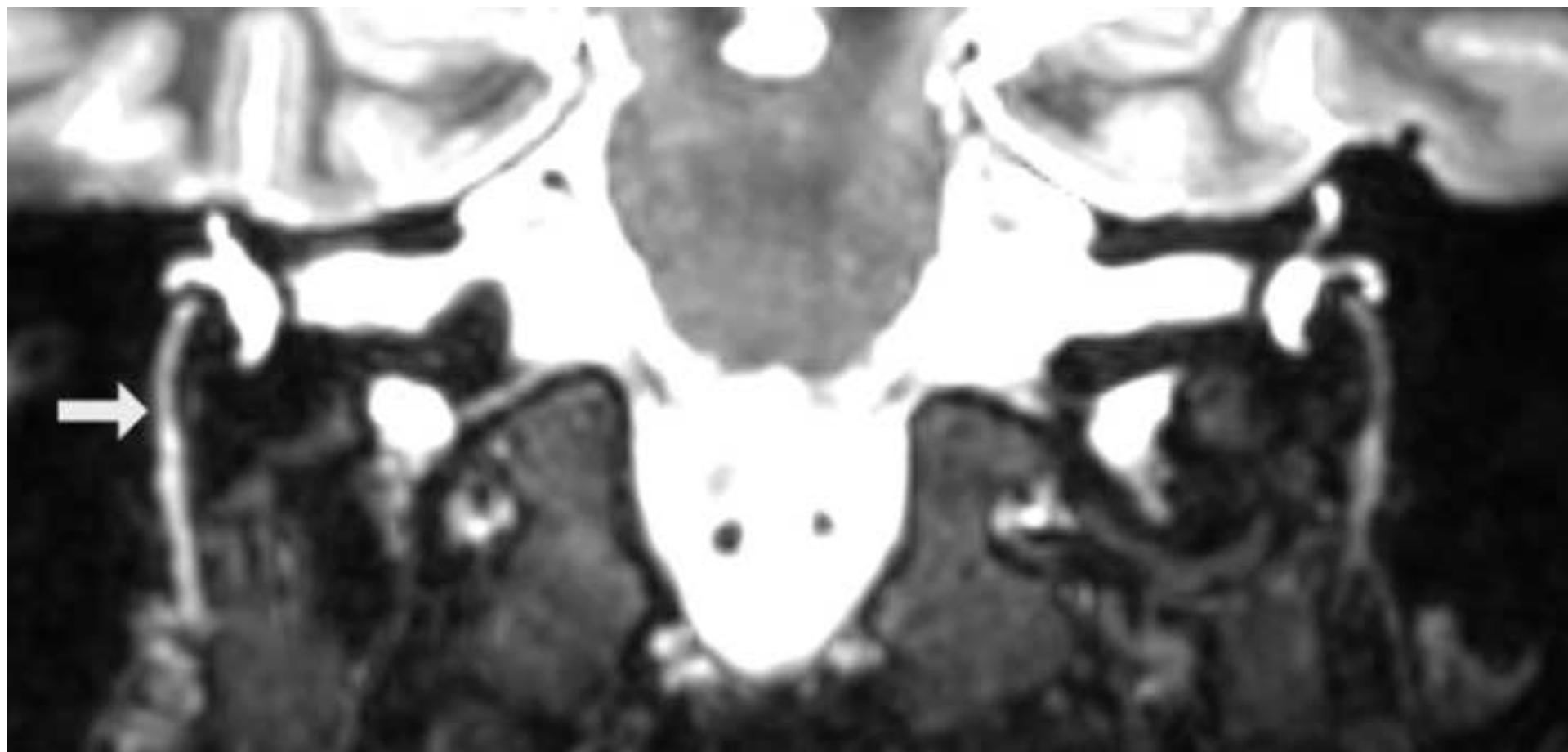


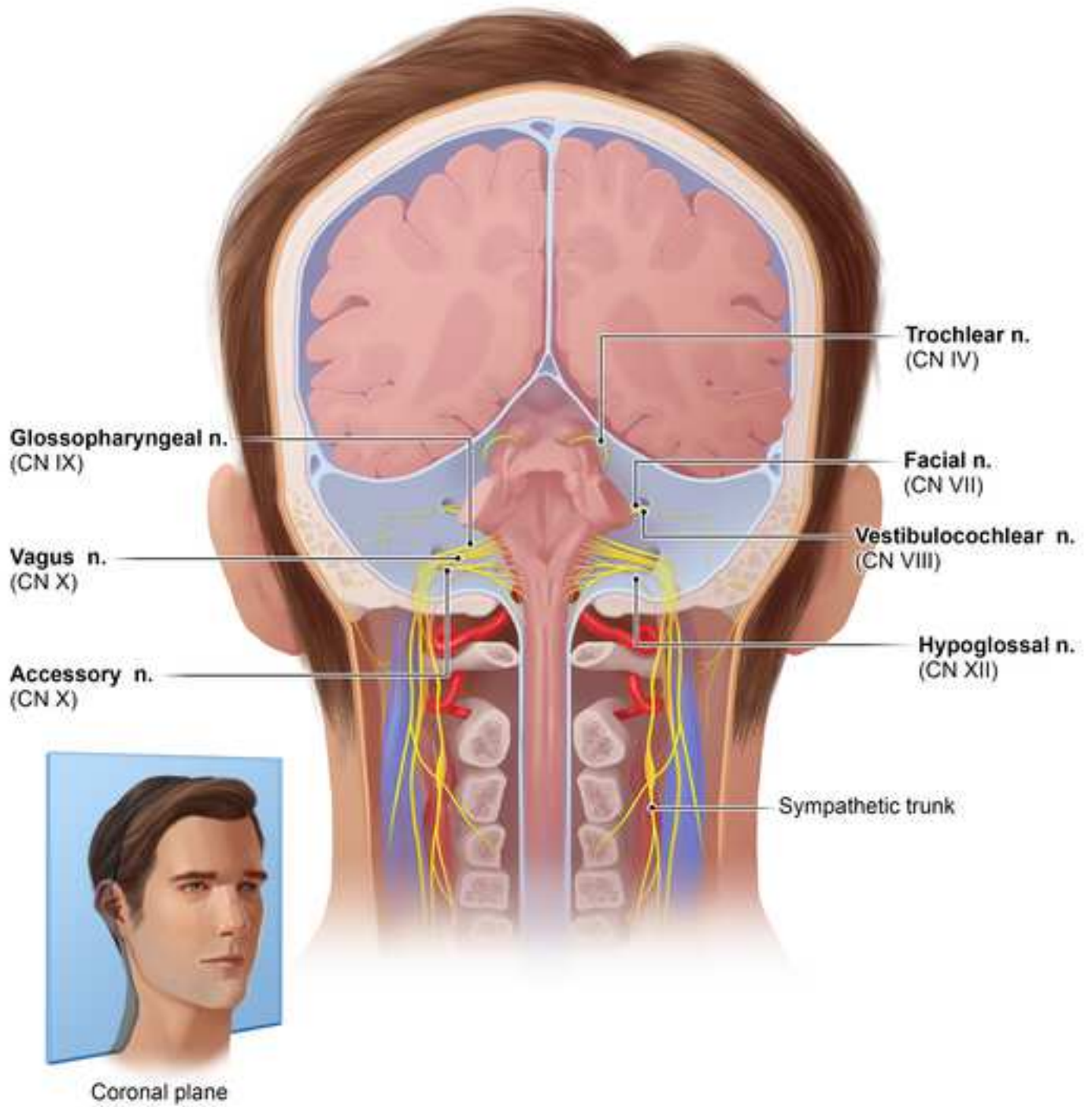


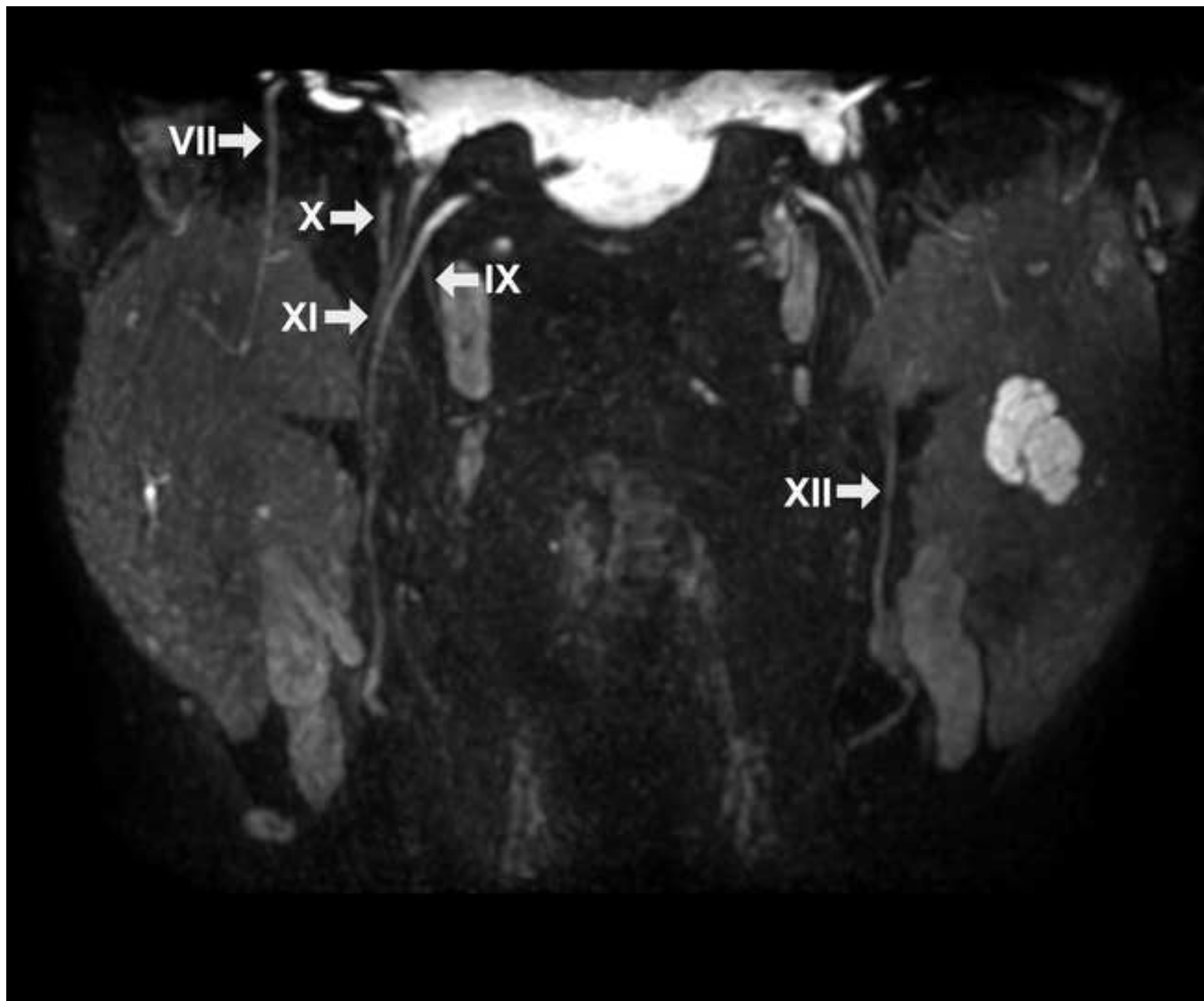


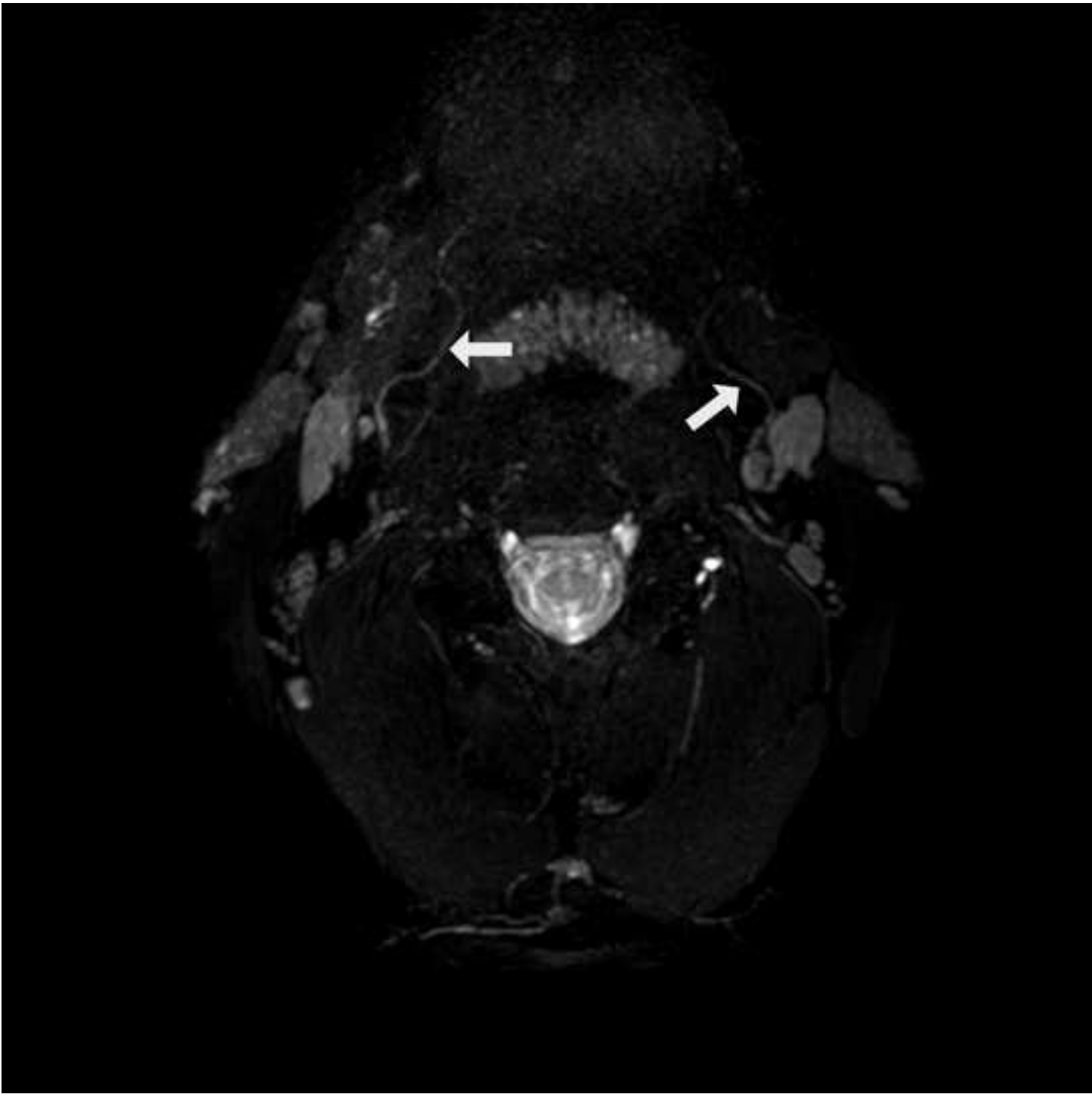


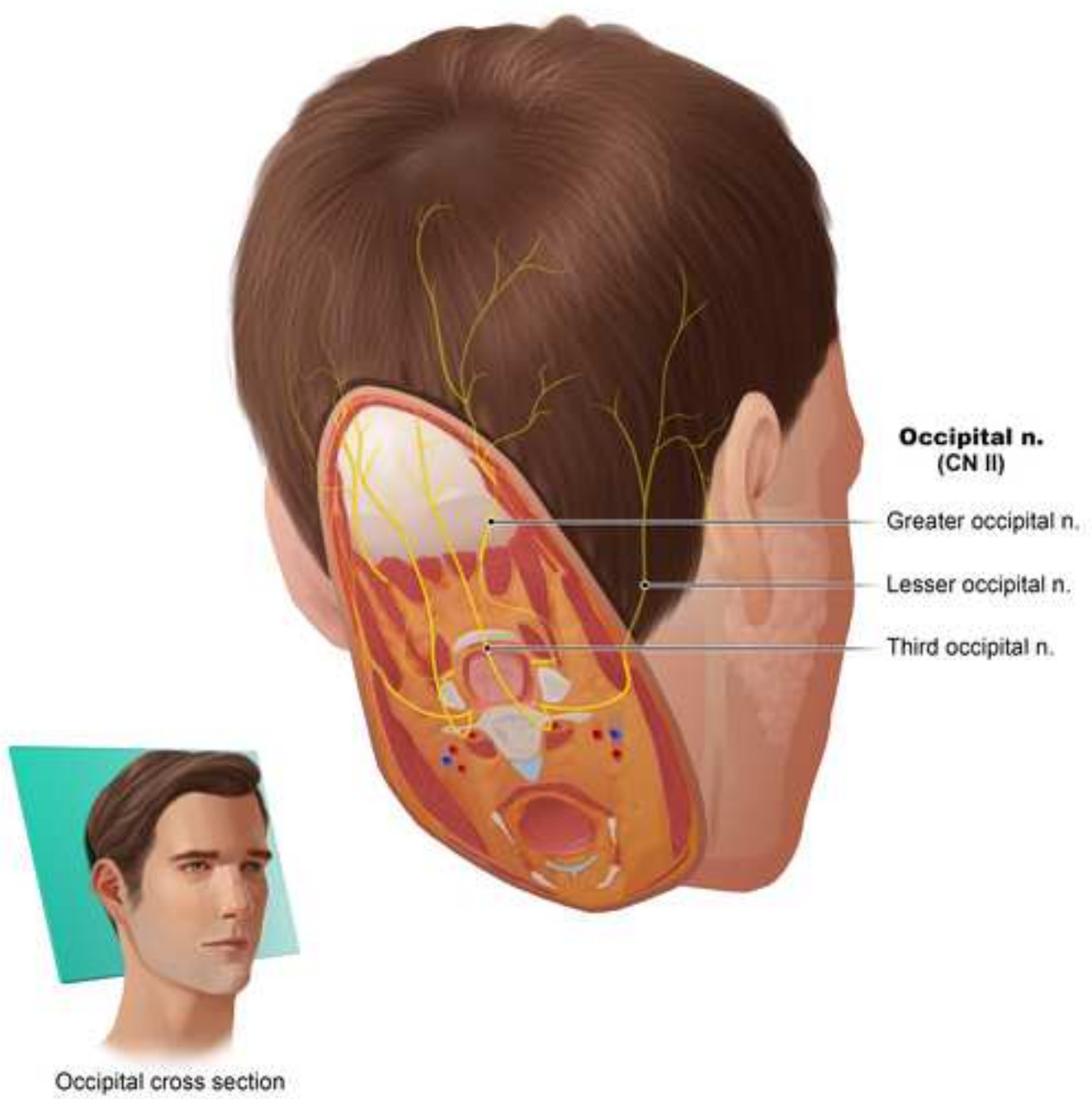


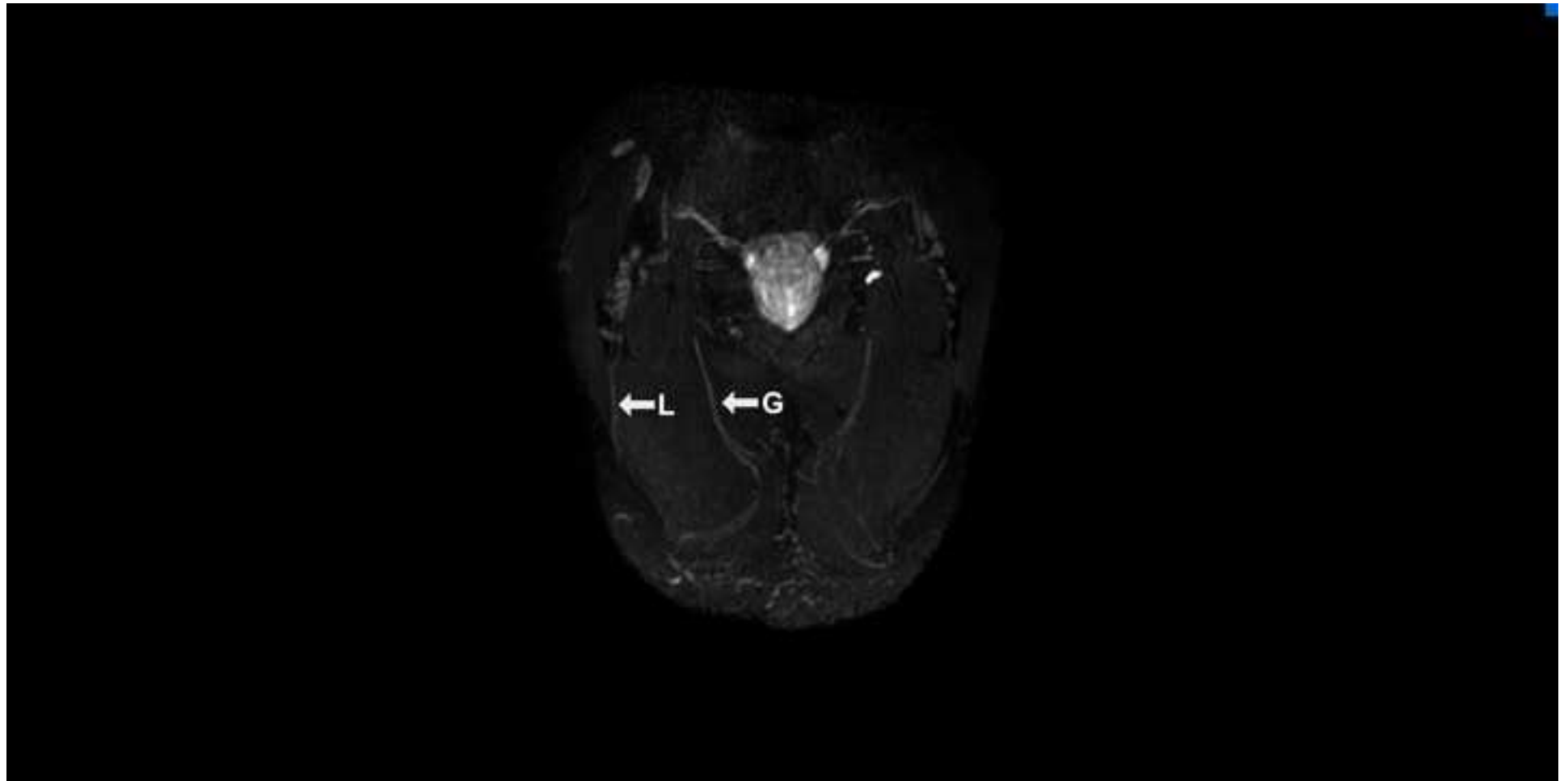














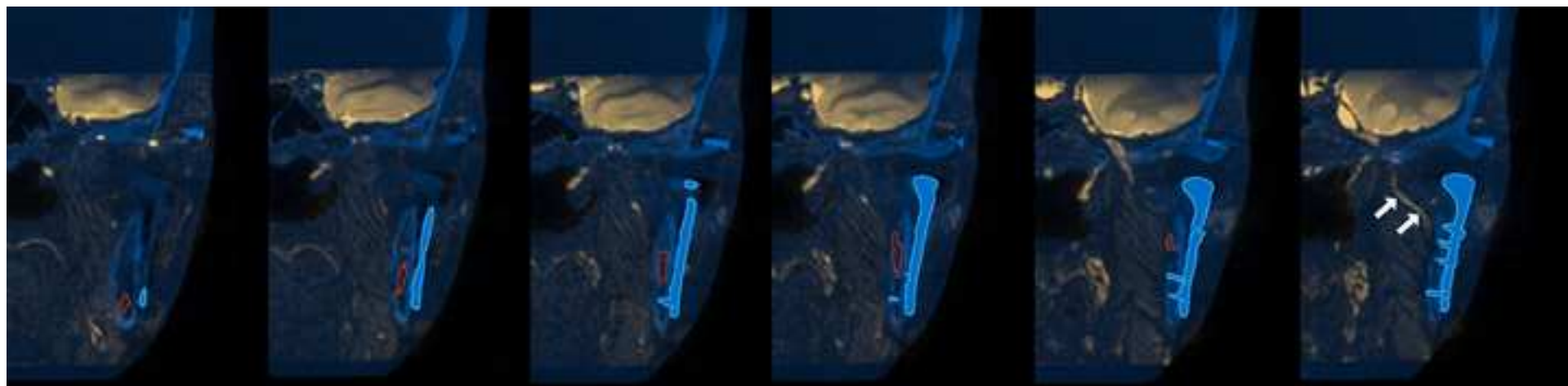


Table 1

	3D CRANI	3D PSIF
Basic MRI technique	3D STIR	3D FFE
TR/TE (msec)	2300/188	12/2.5
Slice thickness (mm)	0.5	0.45
FOV (mm)	200	200
Voxel size (mm)	0.9 isotropic	0.9 isotropic
Acquisition time (min:sec)	5:17	6:45
Compressed sensing	Yes	No
Flip angle	N/A	35°
Fat suppression technique	MSDE	Proset



[Click here to access/download](#)

Supplementary material

Video Magnetic Resonance Neurography 4K.mp4

